**UNIVERSITY OF GAZİANTEP**

**GRADUATE SCHOOL OF**

**NATURAL & APPLIED SCIENCES**


**FREE VIBRATION OF LAMINATED HYBRID COMPOSITE PLATES**


**M. SC. THESIS**

**IN**

**MECHANICAL ENGINEERING**


**BY**

**MEHMET BULUT**

**JUNE 2013**

**Free Vibration of Laminated Hybrid Composite Plates**


**M. Sc. Thesis**

**In**

**Mechanical Engineering**

**University of Gaziantep**


**Supervisor**

**Assist. Prof. Dr. Ahmet ERKLİĞ**


**by**

**Mehmet BULUT**

**June 2013**

REPUBLIC OF TURKEY
UNIVERSITY OF GAZİANTEP
GRADUATE SCHOOL OF NATURAL & APPLIED SCIENCES
MECHANICAL ENGINEERING DEPARTMENT

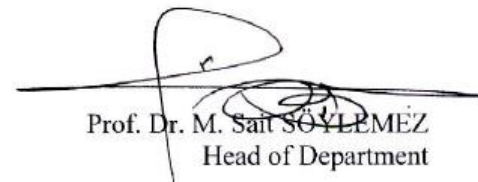Name of thesis: Free Vibration of Laminated Hybrid Composite Plates

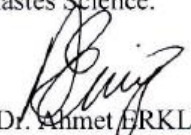Name of the Student: Mehmet Bulut

Exam Date: 26.06.2013

Approval of the Graduate School of Natural and Applied Sciences

Assoc. Prof. Dr. Metin BEDİR
Director

I certify that this thesis satisfies all the requirements as a thesis for the degree of
Master of Science.

Prof. Dr. M. Sait SÖYLEMEZ
Head of Department

This is to certify that we have read this thesis and that in our consensus opinion it is
full adequate, in scope and quality, as a thesis for the degree of Mastes Science.

Asst. Prof. Dr. Ahmet ERKLİĞ
Supervisor

Eximining Committee Members                          Signature

Prof. Dr. İ.Halil GÜZELBEY                  .........................

Prof. Dr. L. Canan DÜLGER                   .........................

Assoc. Prof. Dr. Abdulkadir ÇEVİK           .........................

Asst. Prof. Dr. Mehmet Akif KÜTÜK           .........................

Asst. Prof. Dr. Ahmet ERKLİĞ                .........................

I hereby declare that all information in this document has been obtained and presented in accordance with academic rules and ethical conduct. I also declare that, as required by these rules and conduct, I have fully cited and referenced all material and results that are not original to this work.


Mehmet BULUT

# ABSTRACT

## FREE VIBRATION OF LAMINATED HYBRID COMPOSITE PLATES

**BULUT, MEHMET**
**M. Sc. In Mechanical Engineering**
**Supervisor: Assist. Prof. Dr. Ahmet ERKLİĞ**
**June 2013, 52 Pages**

In this study, effects of fiber types and their arrangements in the lamina on natural frequency and damping properties of laminated hybrid composite plates were investigated. Carbon (C), Kevlar (K) and S-Glass fibers were used as reinforcements. Experimental studies were carried out under the various boundary conditions to determine damping and natural frequencies. Finite element analyses using ANSYS 12.1 software were also performed. Results show that natural frequencies were significantly effected by the fiber types and were increased by using fibers which have higher stiffness in the upper layer. In addition, it was concluded that damping ratio were considerable increased using fibers which have higher viscoelastic properties in the upper layer.

**Keywords:** Natural frequency, hybrid composite plate, damping properties

# ÖZET

## TABAKALI HİBRİT KOMPOZİT PLAKALARIN SERBEST TİTREŞİMİ

**BULUT, MEHMET**
**Yüksek Lisans Tezi, Makine Mühendisliği**
**Tez Yöneticisi: Yrd. Doç. Dr. Ahmet ERKLİĞ**
**Haziran 2013, 52 sayfa**

Bu çalışmada, fiber tipinin ve fiber dizilimlerinin tabakalı hibrit kompozit plakaların doğal frekans ve sönümleme özelliklerine etkileri değişik sınır koşulları altında incelenmiştir. Karbon, Kevlar ve S-Glass fiberler güçlendirici olarak kullanılmıştır. Doğal frekansları ve sönümleme oranlarını tesbit etmek için değişik sınır koşulları altında deneysel çalışmalar yapılmıştır. ANSYS yazılımını kullanarak sonlu elemanlar analizi de gerçekleştirilmiştir. Sonuçlar, fiber tipinin doğal frekans ve sönümleme oranlarına önemli derecede etkisinin olduğu ve üst tabakalarda yüksek rijitlik değerine sahip fiber kulanılmasıyla doğal frekans değerlerinin arttığını göstermektedir. Buna ilaveten, üst tabakalarda akışkanlığı fazla olan fiber kullanılmasıyla sönüm oranları arttığı sonucuna varılmıştır.

**Anahtar kelimeler:** Doğal frekans, hibrit kompozit plaka, sönüm özellikleri

# ACKNOWLEDGEMENT

# CONTENTS

# LIST OF FIGURES

# LIST OF TABLES

## LIST OF SYMBOL

| | |
|---|---|
| $Q$ | Transverse shear force per unit length |
| $M_x, M_y$ | Bending moment resultants per unit length |
| $M_{xy}, M_{yx}$ | Twisting moment resultants per unit length |
| $\varepsilon$ | Plane strain |
| $E$ | Modulus of elasticity |
| $\nu$ | Poisson's ratio |
| $G$ | Shear modulus |
| $\kappa$ | Curvatures of plate mid-surface |
| $D$ | Flexural rigidity of the plate |
| $q$ | Distributed pressure per unit area |
| $V$ | Kelvin-Kirchhoff edge reactions |
| $\omega_{mn}$ | Natural frequency of plate in radian |
| $k^2$ | Non-dimensionless frequency parameter |
| $W$ | Mode shapes of plate |
| $\xi$ | Damping ratio |

# CHAPTER 1

# INTRODUCTION

## 1.1 Background

Composite materials, plastics, and ceramics have been the dominated emerging materials over the last forty years. The volume and number of applications of composite materials has grown steadily, penetrating and conquering new markets relentlessly [1].

A Composite material is a material system composed of two or more macro constituents that differ in shape and chemical composition and which are insoluble in each other. The history of composite materials dates back to early 20th century. In 1940, fiber glass was first used to reinforce epoxy.

A composite material can provide superior and unique mechanical and physical properties because it combines the most desirable properties of its constituents while suppressing their least desirable properties. At present composite materials play a key role in aerospace industry, automobile industry and other engineering applications as they exhibit outstanding strength to weight and modulus to weight ratio. High performance rigid composites made from Glass, Graphite, Kevlar, Boron or Silicon carbide fibers in polymeric matrices have been studied extensively because of their application in aerospace and space vehicle technology. Composite materials offer diverse design requirements with significant weight savings as well as high strength-to-weight ratio as compared to conventional materials. Some advantages of composite materials over conventional one are mentioned below:

- Tensile strength of composites is four to six times greater than that of traditional steel or aluminum.
- Improved torsional stiffness and impact properties
- Higher fatigue endurance limit (up to 60% of the ultimate tensile strength).

1

- 30-45% lighter than aluminum structures designed to the same functional requirements
- Lower embedded energy compared to other structural materials like steel, aluminum etc.
- Composites are less noisy while in operation and provide lower vibration transmission than metals
- Composites are more versatile than metals and can be tailored to meet performance needs and complex design requirements
- Long life offers excellent fatigue, impact, environmental resistance and reduced maintenance
- Composites exhibit excellent corrosion resistance and fire retardancy
- Composite parts can eliminate joints/fasteners, providing part simplification and integrated design compared to conventional metallic parts

There are several types of composite materials. Traditional examples are reinforced concrete, thermoplastics reinforced with short fibers, honeycomb composites, sandwich panels. Some of the most common types of composites are those made of layers, each of these layers is composed of long fibers embedded in a resin. Using various approaches (e.g., mixture theory), each layer can be represented at a macro-scale as an orthotropic material. These laminated composites are widely used in the aerospace industry and are receiving attention in other industries like automotive and medical equipment [2].

Dynamic behavior of laminated composite plates has been intensively studied for many years due to importance of engineering applications. Plates which are subjected to dynamic loading are important parts of automotive, aerospace, marine and bridge structures. Dynamic analysis of composite plates has great importance in scope of transportation vehicles and manufacturing machine structures such as pump cogs, pressure gauge devices and vibration isolation systems.

Hybrid composite is composed of two or more different types of fibers in the same composite structure. It is suitable for development of new composites. For instance, Kevlar has great toughness and low cost, but low compressive strength. However, Graphite has low toughness, but high cost and high compressive strength.

## 1.2 Scope and Outline of the Study

In this study, damping and free vibrations of laminated hybrid composite plates are determined by considering different fiber types and their arrangements in the lamina. Experimental studies are carried out to determine natural frequency and damping properties of laminated hybrid composite plates under the different boundary conditions. Finite element studies are also carried out for validation and for high frequency modes.

Chapter 2 presents a comprehensive literature survey on natural frequency of rectangular plates. Literature survey is given under the three outlines: Free vibration of isotropic plates, free vibration of laminated composite plates and free vibration of laminated hybrid composite plates.

Chapter 3 deals with derivation of fundamental equation for free vibration of isotropic and orthotropic rectangular plate by using Kirchhoff's thin plate theory. Exact solution for free vibration is derived for only simply supported (SS) boundary condition.

Chapter 4 contains experimental results to determine damping and natural frequencies of plates. Hybrid composite plates are produced by hand lay-up method under 0.3 MPa pressure with $80^{0}$C temperature. First two natural frequencies are measured for Clamped-Free-Clamped-Free (C-F-C-F), Clamped-Free-Free-Free (C-F-F-F) and Simply Supported-Free-Simply Supported-Free (SS-F-SS-F) boundary conditions. Half power band-width method is introduced in order to determine damping ratios of hybrid composite plates.

Chapter 5 presents finite element analysis of laminated composite plates to predict mode shapes and natural frequencies at higher modes. ANSYS 12.1 software is used in finite element analysis. Linear layer SHELL 99 element with 40x40 mesh size was used for modeling.

Finally in chapter 6, conclusions drawn from the study are presented.

# CHAPTER 2

# LITERATURE SURVEY

## 2.1 Introduction

Vibration characteristics of isotropic and unisotropic plates are investigated by many researchers because of increasing importance of vibration of plates in engineering applications. In recent years, fiber reinforced materials have been mainly used in engineering applications such as civil, marine and aerospace industry due to their excellent features, such as strength ability, high strength and stiffness to weight ratios. It is required to predict natural frequency and working optimum frequency in structures since system may be failed while working at any natural frequency of the system.

## 2.2 Free vibration of Isotropic Plates

A number of researchers have worked on free vibration analysis of isotropic rectangular plates. Leissa [3] studied free vibration of rectangular isotropic plates under simply supported, free and clamped boundary conditions. Natural frequencies were determined in terms of nondimensional frequency parameters by introducing Ritz method with 36 terms. Exact solution was obtained for only simply supported case.

Liew et al. [4] investigated vibration analysis of shear deformable plates by using Mindlin plate theory. Natural frequencies and mode shapes for moderately thick plates were obtained from eigenvalue equations for different boundary conditions, aspect ratios (length/width) and thickness (thickness/width) ratios .

Moon and Sangbo [5] analyzed free vibtration of rectangular plates with circular and rectangular cutout by using independent coordinate coupling method. Nondimensional frequency parameters and mode shapes for rectangular plates with circular and rectangular cutout were detemined for different boundary conditions.

Warburton [6] introduced the free transverse vibrations of rectangular plates with all possible boundary conditions obtained by combining free, freely-supported, and fixed edges. The Rayleigh method was used to derive a simple approximate frequency expression for all modes of vibration.

Shimpi and Patel [7] investigated free vibration of square and rectangular and isotropic plates under the various boundary conditions. Nondimensional frequency parameters in bending mode were presented for simply supported isotropic square plates.

Bo and Yufeng [8] proposed exact solutions for free vibrations of rectangular plates under the combination of simply supported, clamped and free boundary conditions. Numerical studies were carried out to determine natural frequencies and mode shapes.

Jiu et al. [9] presented solution of free vibrations of rectangular plates by using bessel functions. Classical thin plate theory was used in calculations. Nondimensional frequency parameters and mode shapes of square plate were obtained under different boundary conditions.

## 2.3 Free Vibration of Laminated Composite Plates

Nowadays, materials that are light and high strength have become very popular in the structural design. Manufacturing of composite materials is being able to produce high strength, light weight, high corrosion resistance. Importance of use of the composite materials as structural element are increasing more and more. Previous studies on free vibration of laminated composite plates were presented by many researchers using a variety of approaches [10-22].

Chandrashekhara et al. [10] studied free vibration of symmetrically laminated composite beams and derived exact solutions for free vibration. Rotary inertia and shear deformation effects were taken into account during calculations.

Qatu [11] investigated effects of fiber orientation, edge conditions and material type upon the natural frequency and mode shapes for symmetrically laminated composite plates. Ritz method including algebraic polynomial displacement functions was performed in order to solve vibration problems.

Narita and Leissa [12] studied free vibration of cantilever and rectangular angle-ply and cross-ply laminated composite plates. Natural frequencies were calculated by introducing material and fiber angle. Ritz method was proposed for solution of free vibration problems.

Khdeir and Reddy [13] investigated cross-ply laminated composite beams with arbitrary boundary conditions. An analytical solution of refined beam theory was proposed for solution of free vibration problems.

Khdeir and Reddy [14] developed a complete set of linear equations for free vibration of cross-ply and angle-ply composite plates using second order shear deformation theory and obtained exact analytical solutions for moderately thick and thin plates. Exact solutions were developed for thick, moderately thick, thin plate and plate strips with arbitrary boundary conditions.

Won and Sung [15] studied free and forced vibration analysis of laminated composites. Assumed strain method and constitutive equations were used in the analyses. Exact solutions were given for rectangular and isotropic composite plates.

Aydogdu [16] investigated vibration analysis of angle-ply laminated beams with free, clamped and simply supported edge conditions and combination of them. Natural frequencies were obtained using Ritz method and three degree of freedom shear deformable beam theory.

Mohammed et al. [17] presented dynamic behavior of composite beams. Numerical studies were performed for the prediction of effects of fiber orientation on the natural frequency of composite beam using finite element method. In addition, experimental studies were done for cantilever composite beam made of fiber glass. First two natural frequencies were calculated both using experimental and numerical method.

Cong et al. [18] investigated free vibration of cross-ply laminated composite plates using first order shear deformation theory. Nondimensional frequency values  were

determined with different boundary conditions and with different thickness to width ratios. Effect of cutout on natural frequency and mode shape  was also handled properily.

Erklig et al. [19] studied free vibration of E-Glass polyester composite plates with and without cutouts. Experimental and numerical studies were carried out in order to investigate effects of cutout size and position, aspect ratio of the composite plate under the clamped-free boundary condition.

Turvey et al. [20] investigated natural frequencies of square pultruded GRP plates including effects of anisotropy, hole size ratio and boundary condition. Natural frequencies were determined from experiments with six combinations of clamped, free and simply supported cases, and validated with finite element software NASTRAN

Itishree and Shishir [21] studied free vibration response of woven fiber composite plates under free-free boundary condition. Experimental studies were carried out to determine natural frequencies with different number of layers, aspect ratios and fiber orientations. Finite element studies were also performed in order to validate experimental results.

Rath and Sahu [22] studied vibration behavior of woven fiber laminated composite plates in hydrothermal environment. Experimental and numerical studies were performed in order to investigate effects of moisture and temperature on natural frequencies. Natural frequencies were obtained for different boundary conditions and aspect ratios.

## 2.4 Free vibration of laminated hybrid composite plates

Hybrid composites are constituted of successive layers of fibers with different natures such as Glass fibers, Carbon fibers and Kevlar fibers. They are mainly used as structural element in engineering applications since they allow obtaining optimum mechanical properties. There are few studies on free vibration of hybrid composite plates. Adali and Verijenko [23] studied optimum stacking sequence of symmetric laminated hybrid composites under free vibrations. Graphite/Epoxy for outer layers and Glass/Epoxy for inner layers were used for multilayered hybrid laminates.

Optimum design problems with different fiber angels were studied for evaluation of vibration of hybrid laminates. Moreover, effects of hybridization and aspect ratios of hybrid composites on natural frequencies were investigated.

Idicula et al. [24] studied the dynamic behavior of randomly oriented intimately mixed short banana/sisal hybrid fiber reinforced polyester composites. Besides dynamic behavior of composites such as damping and storage modulus, static and impact properties were handled properly. Banana and sisal fibers were preferred for hybridization in order to select high performance and low cost composites.

Chen [25] derived governing equations for vibration and stability of hybrid composite plates in arbitrary stress states. Rotary inertia and shear effects were taken into consideration. Buckling and natural frequency values were evaluated from derived equations. Glass fiber reinforcement polymer and Aluminum were used as a constituent material. Simply supported case was considered as boundary condition.

Shokrieh and Najafi [26] studied dynamic behavior of metallic reinforcement polymer matrix composite plates experimentally. Glass/epoxy was applied to the aluminum 2024 T-3 in the analysis. Mode shapes and vibration frequency values of the laminated square plates were evaluated for free-free edge condition. First four frequency values were obtained for $[45/0/90/Al]_s$ and $[90/0/+45/-45]_s$ stacking sequences respectively.

Botelho et al. [27] investigated the damping characteristics of continuous fiber/metal composite materials using free vibration method. Carbon/Epoxy, Glass/Epoxy and combination of them with aluminum 2420 were used for dynamic stability of composite plates. Experimental and theoretical studies were performed and compared with each other. First three vibration frequency values were obtained with clamped-free boundary condition.

Chen et al. [28] studied parametric vibrations stability of hybrid composite plates subjected to periodic uniaxial stress and bending stress. Effects of thickness ratio, number of layers, core material, and load parameters on natural frequencies were

examined properly. Graphite/Epoxy, Glass/Epoxy and aluminum materials were used for production of hybrid composite plates.

Khan et al. [29] presented damping properties of composite plates containing carbon nanotube material under the free and forced vibrations. Experimental studies were carried out for prediction of damping ratios under the cantilever boundary condition. Damping ratios of hybrid composites were measured by using Half-power bandwidth method for different content of carbon nanotubes.

## 2.5 Conclusion on Literature Review

The following conclusions were obtained from the literature reviews;

- There are a lot of studies on the natural frequency of laminated composite plates.

- Available literature on damping and free vibration of hybrid composites is fewer.

- The previous studies mentioned here were investigated only the laminated plates with a single material. Especially two types of fibers or fiber-metal hybrid composites were studied with various boundary conditions.

The main goal of this thesis is to investigate the natural frequencies of the hybrid composite plate. The specific objectives are;

- To find the effects of fiber types (carbon, Kevlar and s-glass fibers) on damping and natural frequencies,

- To investigate the effects of boundary conditions such as C-F-C-F, C-F-F-F and SS-F-SS-F boundary conditions.

- To predict numerically natural frequencies of hybrid composite plates in higher modes

# CHAPTER 3

## THEORY OF FREE VIBRATION OF RECTANGULAR PLATES

### 3.1 Introduction

Theoretical formulation for transversely vibrating rectangular plate was obtained by introducing of Kirchhoff assumptions. Following assumptions have been made

- No deformations occur in the midplane of the plate
- Transverse normal stress is not allowed
- Normals to the undeformed plane remain straight and normal to the deformed midplane and unstretched in length
- The effects of rotary inertia is negligible

As can be seen in Figure 3.1, a plate with thickness of $h$ is clamped at one side, simply supported at another side and a third side completely free. Rectangular coordinates are shown, where $x$ and $y$ are in-plane coordinate, and $z$ is transverse coordinate. Coordinate system is located at the mid-plane of the plate, so that bottom and top surfaces of plate are at $z = \pm h/2$ when the plate is in equilibrium. Figure 3.2 shows the sketch of element which is in displaced position and deformed shape. $Q_x$ and $Q_y$ are transverse shearing forces per unit length, $M_x$ and $M_y$ are bending moment resultants per unit length, $M_{xy}$ and $M_{yx}$ are twisting moment resultants per unit length and $q$ is distributed pressure per unit area.
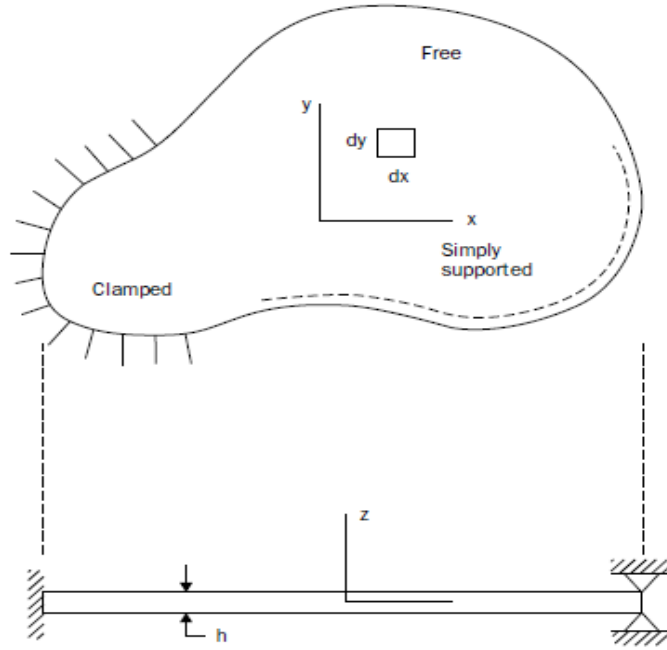
**Figure 3.1** Plate of arbitrary shape and edge conditions [2]
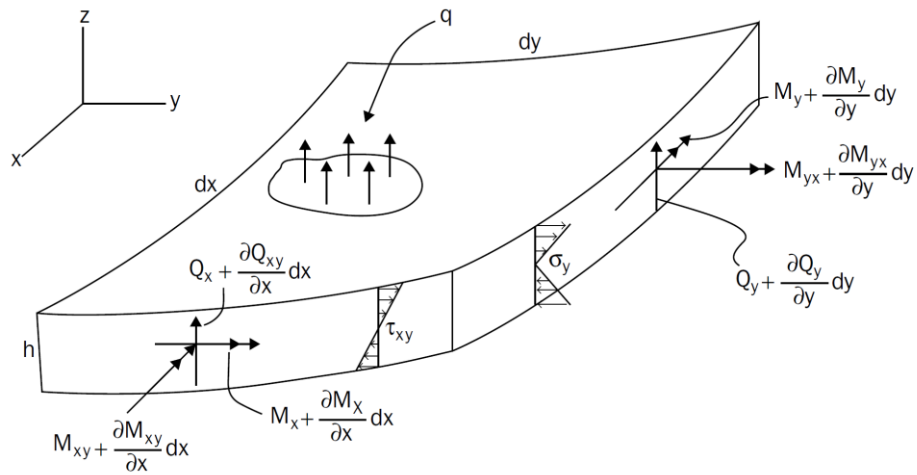


**Figure 3.2** Deformed plate element with forces and moments [2]

Deformed mid-surface of plate is characterized by membrane surface. Displacement in the $z$ direction is $w$, density of plate per unit volume is $\rho$ and distributed force in the $z$ direction is $q$. Summing forces in the $z$ direction yields

$$-Q_x dy + \left(Q_x + \frac{\partial Q_x}{\partial x} dx\right) dy - Q_y + \left(Q_y + \frac{\partial Qy}{\partial y} dy\right) dx + q dx dy = \rho h dx dy \frac{\partial^2 w}{\partial t^2} \qquad (3.1)$$

Summing the moment about an axis parallel to $y$ through to center of the element yields

$$M_x dy - \left(M_x + \frac{\partial M_x}{\partial x} dx\right)dy + M_{yx}dx - \left(M_{yx} + \frac{\partial M_{yx}}{\partial y} dy\right)dx + Q_x dy \frac{dx}{2} +$$
$$\left(Q_x + \frac{\partial Q_x}{\partial x} dx\right)dy \frac{dx}{2} = \rho\left(\frac{h^3}{12} dxdy\right)\left(\frac{\partial^2}{\partial t^2}\left(\frac{\partial w}{\partial x}\right)\right)$$
$$(3.2)$$

After dropping higher order terms involving $\frac{\partial Q_x}{\partial x}$, from equation (3.1) and (3.2) yields

$$Q_x - \frac{\partial M_x}{\partial x} - \frac{\partial M_{xy}}{\partial y} = 0 \tag{3.3}$$

$$Q_y - \frac{\partial M_{xy}}{\partial x} - \frac{\partial M_y}{\partial y} = 0 \tag{3.4}$$

Displacements in x and y directions are given as $u$ and $v$ respectively.

$$u = -z\frac{\partial w}{\partial x}, \qquad v = -z\frac{\partial w}{\partial y} \tag{3.5}$$

Plane strains obtained from $u$ and $v$ displacement components are as follows

$$\varepsilon_x = \frac{\partial u}{\partial x}, \quad \varepsilon_y = \frac{\partial v}{\partial y}, \quad \gamma_{xy} = \frac{\partial u}{\partial y} + \frac{\partial v}{\partial x} \tag{3.6}$$

Substituting (3.5) into the (3.6) yields

$$\varepsilon_x = -z\frac{\partial^2 w}{\partial x^2}, \varepsilon_y = -z\frac{\partial^2 w}{\partial y^2}, \quad \gamma_{xy} = -2z\frac{\partial^2 w}{\partial x \partial y} \tag{3.7}$$

Stress and strain relationship can be written as follows

$$\varepsilon_x = \frac{1}{E}\left(\sigma_x - v\sigma_y\right), \varepsilon_y = \frac{1}{E}\left(\sigma_y - v\sigma_x\right), \gamma_{xy} = \frac{\tau_{xy}}{G} \tag{3.8}$$

Where $E$ is modulus of elasticity, $v$ is Poisson's ratio and $G$ is the shear modulus. Bending moments are derived by integrating the moments of in-plane stresses over the plate thickness.

$$M_x = \int_{-h/2}^{h/2} \sigma_x z\, dz, \, M_y = \int_{-h/2}^{h/2} \sigma_y z\, dz, \, M_{xy} = \int_{-h/2}^{h/2} \tau_{xy} z\, dz \qquad (3.9)$$

From equation (3.8) and (3.9), curvature moments are

$$M_x = -D(\kappa_x + v\kappa_y), \, M_y = -D(\kappa_y + v\kappa_x), \, M_{xy} = -D(1-v)\kappa_{xy} \qquad (3.10)$$

$$\kappa_x = \frac{\partial^2 w}{\partial x^2}, \kappa_y = \frac{\partial^2 w}{\partial x^2}, \, \kappa_{xy} = \frac{\partial^2 w}{\partial x \partial y} \qquad (3.11)$$

Where $\kappa_x$, $\kappa_y$ and $\kappa_{xy}$ are curvatures of plate mid-surfaces, and $D$ is flexural rigidity of the plate.

$$D = \frac{Eh^3}{12(1-v)} \qquad (3.12)$$

Equation (3.13) is obtained from (3.3), (3.4) and (3.2) as follows

$$\frac{\partial^2 M_x}{\partial x^2} + \frac{\partial^2 M_y}{\partial y^2} + 2\frac{\partial^2 M_{xy}}{\partial x \partial y} + q = \rho h \frac{\partial^2 w}{\partial t^2} \qquad (3.13)$$

Substituting (3.10) and (3.11) into the (3.12) gives

$$D\left(\frac{\partial^2 w}{\partial x^2} + \frac{\partial^2 w}{\partial y^2} + 2\frac{\partial^2 w}{\partial x \partial y}\right) + \rho h \frac{\partial^2 w}{\partial t^2} = q \qquad (3.14)$$

And the other form of equation (3.13) as follows [31]

$$D\nabla^4 w + \rho h \frac{\partial^2 w}{\partial t^2} = q \qquad (3.15)$$

Shear forces in the x- and y- axes are defined as

$$V_x = Q_x + \frac{\partial M_{xy}}{\partial y} \text{ and } V_y = Q_y + \frac{\partial M_{xy}}{\partial x} \qquad (3.16)$$

Another form of equation (3.16) is given as follows

$$V_x = -D\left[\frac{\partial^3 w}{\partial x^3} + (2-v)\frac{\partial^3 w}{\partial x \partial y^2}\right], \, V_y = -D\left[\frac{\partial^3 w}{\partial y^3} + (2-v)\frac{\partial^3 w}{\partial x^2 \partial y}\right] \qquad (3.17)$$

## 3.2 Simply Supported Rectangular Plate Along Two Opposing Edges

It is assumed that two opposite sides are simply supported where $x = 0$ and $x = a$, other sides may be clamped, simply supported, or free as shown in the Figure 3.3. $q$ is zero under the free and undamped vibration. So governing equation is written as

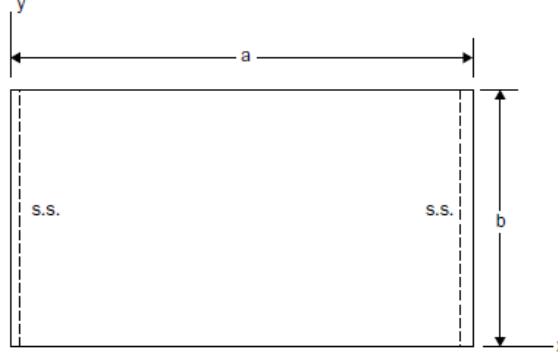$$D\nabla^4 w + \rho h \frac{\partial^2 w}{\partial t^2} = q \tag{3.18}$$

**Figure 3.3** Simply supported rectangular plate with opposite sides simply supported (SS-F-SS-F) boundary condition

Approximate function of $w(x,y,t)$ is chosen as follows

$$w(x, y, t) = W(x, y)\sin(\omega t) \tag{3.19}$$

By substituting equation (3.19) into equation (3.18) gives

$$(\nabla^4 - k^4)W = 0 \tag{3.20}$$

Where $k^4 = \rho h \omega^2 / D$. Solution of equation (3.20) was obtained by summing solutions of two parts of equation (3.20)

$$(\nabla^2 + k^2)W_1 = 0 \tag{3.21}$$

$$(\nabla^2 - k^2)W_1 = 0 \tag{3.22}$$

Final solution is obtained by addition of equations of (3.21) and (3.22)

$$W = W_1 + W_2 = 0 \tag{3.23}$$

Functions of $W_1$ and $W_2$ are seperated in two parts as

$$W_1(x, y) = X_1(x)Y_1(y) \tag{3.24}$$

$$W_2(x, y) = X_2(x)Y_2(y) \tag{3.25}$$

Ordinary differential equation can be written as

$$Y_1 \frac{d^2 X_1}{dx^2} + X_1 \frac{d^2 Y_1}{dy^2} + X_1 Y_1 k^2 = 0 \tag{3.26}$$

By separation of variable into the two parts yields

$$\frac{d^2 X_1}{dx^2} + \alpha_1^2 X_1 = 0 \tag{3.27}$$

$$\frac{d^2 Y_1}{dy^2} + \alpha_2^2 Y_1 = 0 \tag{3.28}$$

Where;

$$k^2 = \alpha_1^2 + \alpha_2^2 \tag{3.29}$$

Solution of second order differential equation (3.27) and (3.28) are expressed in the form of approximate functions given as follows [30]

$$X_1(x) = A' \sin(\alpha_1 x) + B' \cos(\alpha_1 x) \tag{3.30}$$

$$Y_1(x) = C' \sin(\alpha_2 y) + D' \cos(\alpha_2 y) \tag{3.31}$$

Substituting (3.30) and (3.31) into the (3.22) gives

$$\begin{aligned} W_1(x, y) &= \left(A' \sin(\alpha_1 x) + B' \cos(\alpha_1 x)\right)\left(C' \sin(\alpha_2 y) + D' \cos(\alpha_2 y)\right) \\ &= A \sin(\alpha_1 x) \sin(\alpha_2 y) + B \sin(\alpha_1 x) \cos(\alpha_2 y) + \\ &\quad C \cos(\alpha_1 x) \sin(\alpha_2 y) + D \cos(\alpha_1 x) \cos(\alpha_2 y) \end{aligned} \tag{3.32}$$

Where $A = A'C'$, $B = A'D'$, $C = B'C'$, $D = B'D'$. Similarly, by substitution of (3.25) into the equation (3.22) yields

$$X_2(x) = E' \sinh \alpha_1 x + F' \cosh \alpha_1 x \tag{3.33}$$

15

$$Y_2(y) = G' \sinh \alpha_2 x + H' \cosh \alpha_2 x \tag{3.34}$$

From equation (3.25), (3.33) and (3.34), $W_2(x, y)$ was derived as follows

$$\begin{aligned} W_2(x, y) &= E \sin(\alpha_1 x) \sin(\alpha_2 y) + F \sin(\alpha_1 x) \cos(\alpha_2 y) + \\ & G \cos(\alpha_1 x) \sin(\alpha_2 y) + H \cos(\alpha_1 x) \cos(\alpha_2 y) \end{aligned} \tag{3.35}$$

Solution of $W(x, y)$ was derived from equation (3.32) and (3.35)

$$\begin{aligned} W(x, y) &= A \sin(\alpha_1 x) \sin(\alpha_2 y) + B \sin(\alpha_1 x) \cos(\alpha_2 y) + \\ & C \cos(\alpha_1 x) \sin(\alpha_2 y) + D \cos(\alpha_1 x) \cos(\alpha_2 y) + \\ & E \sinh(\alpha_1 x) \sinh(\alpha_2 y) + F \sinh(\alpha_1 x) \cosh(\alpha_2 y) + \\ & G \cosh(\alpha_1 x) \sinh(\alpha_2 y) + H \cos(\alpha_1 x) \cosh(\alpha_2 y) \end{aligned} \tag{3.36}$$

Constants $A$, $B$, $C$, $D$, $E$, $F$, $G$ and $H$ depend on edge condition of the plate applied to the edges. Exact solution of equation (3.36) is resulted in simply supported case by the application of boundary condition as follows

$$\text{if } x = 0 \text{ and } x = a, W = \frac{\partial^2 w}{\partial x^2} = 0 \tag{3.37}$$

$$\text{if } y = 0 \text{ and } y = b, W = \frac{\partial^2 w}{\partial y^2} = 0 \tag{3.38}$$

Solution of x-coordinate is derived by separating equation (3.32) in the two parts

$$\begin{aligned} \overline{W}(x) &= X_1(x) + X_2(x) \\ &= A' \sin(\alpha_1 x) + B' \cos(\alpha_1 x) + E' \sinh(\alpha_1 x) + F' \cosh(\alpha_1 x) \end{aligned} \tag{3.39}$$

Second derivative of (3.39) is derived as

$$\begin{aligned} W''(x) &= \frac{\partial^2 W}{\partial x^2} = -A' \alpha_1^2 \sin \alpha_1 x - B' \alpha_1^2 \cos \alpha_1 x + E' \alpha_1^2 \sinh \alpha_1 x \\ & + F' \alpha_1^2 \cosh \alpha_1 x \end{aligned} \tag{3.40}$$

By applying boundary condition $\overline{W}(0) = 0$ and $\overline{W}(a) = 0$ in equation (3.39) yields

$$B' + F' = 0 \tag{3.41}$$

16

$$A' \sin \alpha_1 a + B' \cos \alpha_1 a + E' \sinh \alpha_1 a + F' \cosh \alpha_1 a \tag{3.42}$$

And putting (3.42) into the (3.39) $W''(0) = W''(a) = 0$ yields

$$-\alpha_1^2 B' + \alpha_2^2 F' = 0 \tag{3.43}$$

$$-A'\alpha_1^2 \sin \alpha_1 a - B'\alpha_1^2 \cos \alpha_1 a + E'\alpha_1^2 \sinh \alpha_1 a + F'\alpha_1^2 \cosh \alpha_1 a \tag{3.44}$$

As can be seen from equation (3.41) and (3.44) $B' = F' = 0$, since $\alpha_1^2 \neq 0$

$$A' \sin \alpha_1 a + E' \sinh \alpha_1 a = 0 \tag{3.45}$$

$$-A'\alpha_1^2 \sin \alpha_1 a + E'\alpha_1^2 \sinh \alpha_1 a = 0 \tag{3.46}$$

Equation (3.45) yields

$$-A' \sin \alpha_1 a = E' \sinh \alpha_1 a \tag{3.47}$$

Substituting (3.47) into the (3.46) gives

$$A' \sin \alpha_1 a = 0 \tag{3.48}$$

From equation (3.47) and (3.48), it is concluded that $E' = 0$ since $\sinh \alpha_1 a \neq 0$

So, $\overline{W}(x)$ is written as

$$\overline{W}(x) = A' \sin \alpha_1 a \tag{3.49}$$

From equation (3.48) $A' \neq 0$ and

$$\sin \alpha_1 a = 0 \tag{3.50}$$

From equation (3.50)

$$\alpha_1 = \frac{m\pi}{a} \tag{3.51}$$

Where $m$=0, 1, 2, 3…

Equations (3.41), (3.42), (3.43) and (3.44) are written in the form of matrix as

17

$$
\begin{bmatrix}
0 & 1 & 0 & 1 \\
\sin\alpha_1 a & \cos\alpha_1 a & \sinh\alpha_1 a & \cosh\alpha_1 a \\
0 & -\alpha_1^2 & 0 & \alpha_1^2 \\
-\alpha_1^2\sin\alpha_1 a & -\alpha_1^2\cos\alpha_1 a & \alpha_1^2\sinh\alpha_1 a & \alpha_1^2\cosh\alpha_1 a
\end{bmatrix}
\begin{bmatrix}
A' \\ B' \\ E' \\ F'
\end{bmatrix}
=
\begin{bmatrix}
0 \\ 0 \\ 0 \\ 0
\end{bmatrix}
\tag{3.52}
$$

Determinant of the above matrix is equal to zero for the satisfaction of equation (3.52) and could be solved using MATHEMATICA software. When expanding the matrix, it is concluded that one equation is directly written as

$$
\sin\alpha_1 a\,\sinh\alpha_1 a = 0
\tag{3.53}
$$

$\sin\alpha_1 a = 0$, since $\sinh\alpha_1 a \neq 0$. So, $\alpha_1 = \dfrac{m\pi}{a}$ and $m = 0, 1, 2 \ldots$

Similarly, solution of y-coordinate is derived from equation (3.31) and (3.34)

$$
\begin{aligned}
\overline{W}(y) &= Y_1(y) + Y_2(y) \\
&= C'\sin\alpha_2 y + D'\cos\alpha_2 y + G'\sinh\alpha_2 y + H'\cosh\alpha_2 y
\end{aligned}
\tag{3.54}
$$

$\overline{W}(y)$ can be written as

$$
\overline{W}(y) = C'\sin\alpha_2 b
\tag{3.55}
$$

Where $C' \neq 0$, so

$$
\sin\alpha_2 b = 0
\tag{3.56}
$$

From equation (3.56)

$$
\alpha_2 = \frac{n\pi}{b}
\tag{3.57}
$$

Where $n = 0, 1, 2, 3\ldots.$

As a result, $W(x, y)$ is expressed as follows by combining equation (3.55) and (3.49)

$$
W(x, y) = A\sin\alpha_1 x\,\sin\alpha_2 y
\tag{3.58}
$$

Where $A = A'C'$

Substituting values of $\alpha_1$ and $\alpha_2$ in the equation (3.29) gives

$$k^2 = \omega_{mn} \sqrt{\frac{\rho h}{D}} = \pi^2 \left[ \left(\frac{m}{a}\right)^2 + \left(\frac{n}{b}\right)^2 \right]$$

(3.59)

Where $k^2$ was the non-dimensionless frequency parameters ($\omega_{mn}$)

$$\omega_{mn} = \pi^2 \left[ \left(\frac{m}{a}\right)^2 + \left(\frac{n}{b}\right)^2 \right] \sqrt{\frac{D}{\rho h}}$$

(3.60)

And also equation (3.58) can be written as

$$W(x, y) = A \sin\frac{m\pi x}{a} \sin\frac{n\pi y}{b}$$

(3.61)

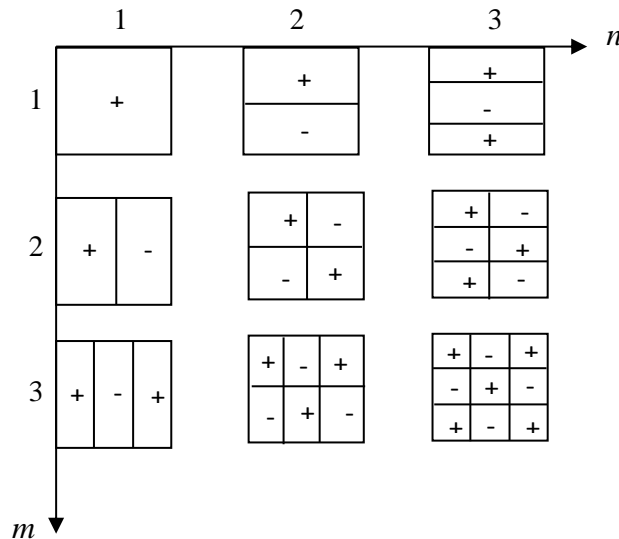Mode shapes of a simply supported square plate is shown in the Figure 3.4



**Figure 3.4** Mode shapes of a simply supported square plate [31]

Non-dimensionless frequency parameters corresponding to mode shapes for a rectangular plate are given in the Table 3.1

**Table 3.1** Non-dimensional vibration frequencies for SS-F-SS-F case [31]

| $m$ | $n$ | |
|---|---|---|
| | 1 | 2 |
| 1 | 19.72 | 49.30 |
| 2 | 49.30 | 78.88 |

## 3.3 Two Opposite Sides Clamped

Non-dimensionless frequency parameters are obtained by the application of clamped-clamped boundary as follows

$$if \ x = 0 \ and \ x = a, \frac{\partial W}{\partial x} = 0 \tag{3.62}$$

$$if \ y = 0 \ and \ y = b, \frac{\partial^2 W}{\partial y^2} = \frac{\partial^3 W}{\partial y^3} = 0 \tag{3.63}$$

$$\overline{W}(x) = A'\sin(\alpha_1 x) + B'\cos(\alpha_1 x) + E'\sinh(\alpha_1 x) + F'\cosh(\alpha_1 x) \tag{3.64}$$

$$\overline{W}(y) = C'\sin\alpha_2 y + D'\cos\alpha_2 y + G'\sinh\alpha_2 y + H'\cosh\alpha_2 y \tag{3.65}$$

By substitution of (3.64) into the boundary condition of (3.62) yields

$$B' + F' = 0 \tag{3.66}$$

$$A'\alpha_1 + E'\alpha_1 = 0 \tag{3.67}$$

$$A'\sin(\alpha_1 a) + B'\cos(\alpha_1 a) + E'\sinh(\alpha_1 a) + F'\cosh(\alpha_1 a) = 0 \tag{3.68}$$

$$A'\alpha_1 \cos\alpha_1 a - B'\alpha_1 \sin\alpha_1 a + E'\alpha_1 \cosh\alpha_1 a + F'\alpha_1 \sinh\alpha_1 a \tag{3.69}$$

$$\begin{bmatrix} 0 & 1 & 0 & 1 \\ \sin\alpha_1 a & \cos\alpha_1 a & \sinh\alpha_1 a & \cosh\alpha_1 a \\ \alpha_1 & 0 & \alpha_1 & 0 \\ \alpha_1 \cos\alpha_1 a & -\alpha_1 \sin\alpha_1 a & \alpha_1 \cosh\alpha_1 a & \alpha_1 \sinh\alpha_1 a \end{bmatrix} \begin{bmatrix} A' \\ B' \\ E' \\ F' \end{bmatrix} = \begin{bmatrix} 0 \\ 0 \\ 0 \\ 0 \end{bmatrix} \tag{3.70}$$

Equation (3.70) is satisfied when the determinant of matrix is equal to zero. After the expanding the matrix and result is directly written as

20

$$\cos(\alpha_1 a)\cosh(\alpha_1 a) - 1 = 0 \tag{3.71}$$

Similarly, solution of y-coordinate is obtained by applying boundary condition of (3.62)

$$\overline{W}(y) = C'\sin\alpha_2 y + D'\cos\alpha_2 y + G'\sinh\alpha_2 y + H'\cosh\alpha_2 y \tag{3.72}$$

$$\overline{W}'(y) = \alpha_2 C'\cos\alpha_2 y - \alpha_2 D'\sin\alpha_2 y + \alpha_2 G'\cosh\alpha_2 y + \alpha_2 H'\sinh\alpha_2 y \tag{3.73}$$

$$\overline{W}''(y) = -\alpha_2^2 C'\sin\alpha_2 y - \alpha_2^2 D'\cos\alpha_2 y + \\ \alpha_2^2 G'\cosh\alpha_2 y + \alpha_2^2 H'\sinh\alpha_2 y \tag{3.74}$$

$$\overline{W}'''(y) = -\alpha_2^3 C'\sin\alpha_2 y + \alpha_2^3 D'\cos\alpha_2 y + \\ \alpha_2^3 G'\sinh\alpha_2 y + \alpha_2^3 H'\cosh\alpha_2 y \tag{3.75}$$

$$-D'\alpha_2^2 + H'\alpha_2^2 = 0 \tag{3.76}$$

$$C'\alpha_2^3 + G'\alpha_2^3 = 0 \tag{3.77}$$

$$-\alpha_2^2 C'\sin\alpha_2 b - \alpha_2^2 D'\cos\alpha_2 b + \alpha_2^2 G'\cosh\alpha_2 b + \alpha_2^2 H'\sinh\alpha_2 b = 0 \tag{3.78}$$

$$-\alpha_2^3 C'\sin\alpha_2 b + \alpha_2^3 D'\cos\alpha_2 b + \alpha_2^3 G'\sinh\alpha_2 b + \alpha_2^3 H'\cosh\alpha_2 b = 0 \tag{3.79}$$

Equations of (3.76), (3.77), (3.78) and (3.79) are expressed in the form of matrix

$$\begin{bmatrix} 0 & -\alpha_2^2 & 0 & \alpha_2^2 \\ \alpha_2^3 & 0 & \alpha_2^3 & 0 \\ -\alpha_2^2\sin\alpha_2^2 b & -\alpha_2^2\cos\alpha_2^2 b & \alpha_2^2\cosh\alpha_2^2 b & \alpha_2^2\sinh\alpha_2^2 b \\ -\alpha_2^3\sin\alpha_2^3 & \alpha_2^3\cos\alpha_2^3 & \alpha_2^3\sinh\alpha_2^3 & \alpha_2^3\cosh\alpha_2^3 \end{bmatrix} \begin{bmatrix} C' \\ D' \\ G' \\ H' \end{bmatrix} = \begin{bmatrix} 0 \\ 0 \\ 0 \\ 0 \end{bmatrix} \tag{3.80}$$

Determinant of above matrix is equal to zero for the satisfaction of equation of (3.80). After the expanding matrix, values of $\alpha_2$ is solved by using following equation

$$-\alpha_2^{10}\sinh(\alpha_2^2 b)\sinh(\alpha_2^3 b) + \alpha_2^{10}\cosh(\alpha_2^2 b)\cosh(\alpha_2^3 b) - \\ \alpha_2^{10}\sinh(\alpha_2^3 b)\sinh(\alpha_2^2 b) + \alpha_2^{10}\sinh(\alpha_2^2 b)\cos(\alpha_2^3 b) + \alpha_2^{10}\sin(\alpha_2^3 b)\cos(\alpha_2^2 b) + \\ \alpha_2^{10}\cos(\alpha_2^2 b)\sin(\alpha_2^3 b) + \alpha_2^{10}\cosh(\alpha_2^2 b)\cos(\alpha_2^3 b) + \alpha_2^{10}\sin(\alpha_2^2 b)\cosh(\alpha_2^3 b) = 0 \tag{3.81}$$

$\alpha_1$ and $\alpha_2$ values are non-dimensionless frequency parameters and may be obtained by the solution of roots of the above equation. Governing equation for free vibration of square plates is derived as given in equation (3.82). Non-dimensionless frequency parameters for a square plate under the C-F-C-F boundary condition are given in Table 3.2

$$\beta^2 = \alpha_1^2 + \alpha_2^2 = \omega_{mn}a^2\sqrt{\frac{D}{\rho h}}$$
(3.82)

**Table 3.2** Non-dimensional vibration frequencies for C-F-C-F case [31]

| $m$ | $n$ | |
|---|---|---|
| | 1 | 2 |
| 1 | 22.272 | 26.529 |
| 2 | 61.466 | 67.549 |

## 3.4 Vibration of Orthotropic Plate

Plate stiffness and compliance equations for a rectangular shaped plate with dimensions of $a$ (width), $b$ (length) and $h$ (thickness) are derived by considering Kirchhoff's plate theory assumptions under the plane stress condition. Force and moment resultants and lamina coordinates of composite plate were shown in the Figure 3.5 and Figure 3.6
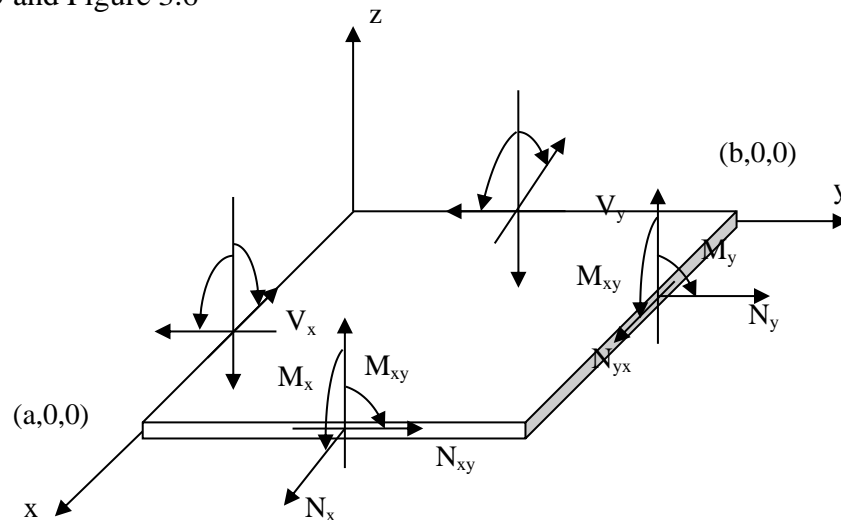


**Figure 3.5** Force and moment resultants on a flat plate

22

Where;

$N_x$ and $N_y$ are forces in the x- and y- directions, $M_x$ and $M_y$ are moment in the x- and y- directions and $V_x$ and $V_y$ are shear forces in the z- direction. Strains of any point in the plate are presented here as a function of displacements

$$\varepsilon_x(x, y, z) = \frac{\partial u_0}{\partial x} - z\frac{\partial \phi_x}{\partial x}$$
(3.83)

$$\varepsilon_y(x, y, z) = \frac{\partial v_0}{\partial y} - z\frac{\partial \phi_y}{\partial y}$$
(3.84)

$$\gamma_{xy}(x, y, z) = \frac{\partial u_0}{\partial y} + \frac{\partial v_0}{\partial x} - z(\frac{\partial \phi_x}{\partial y} + \frac{\partial \phi_y}{\partial y})$$
(3.85)

Where $u_0$, $v_0$ and $w_0$ are displacements along the x-, y- and z- directions, $\phi_x$ and $\phi_y$ are rotation angles after the deformation, $\gamma_{xy}(x, y)$ is shear strain in the x-y plane and $\varepsilon_x(x, y, z)$, $\varepsilon_x(x, y, z)$ and $\varepsilon_x(x, y, z)$ are strains at any point.

Middle surface strains are

$$\varepsilon_x^0(x, y) = \frac{\partial u_0}{\partial x}$$
(3.86)

$$\varepsilon_y^0(x, y) = \frac{\partial v_0}{\partial y}$$
(3.87)

$$\gamma_{xy}^0(x, y) = \frac{\partial u_0}{\partial y} + \frac{\partial v_0}{\partial x}$$
(3.88)

Strains at any point in the plate can be written as follows [31]

$$\begin{Bmatrix} \varepsilon_x \\ \varepsilon_y \\ \gamma_{xy} \end{Bmatrix} = \begin{Bmatrix} \varepsilon_x^0 \\ \varepsilon_y^0 \\ \gamma_{xy}^0 \end{Bmatrix} + z\begin{Bmatrix} \kappa_x \\ \kappa_y \\ \kappa_{xy} \end{Bmatrix}$$
(3.89)

Where $\kappa_x$ and $\kappa_y$ are curvature of the plate due to bending, $\kappa_{xy}$ ias curvature of the plate due to twisting and $\varepsilon_x^0$, $\varepsilon_y^0$ and $\gamma_{xy}^0$ are middle surface strains which presents the stretching and shear of the plate
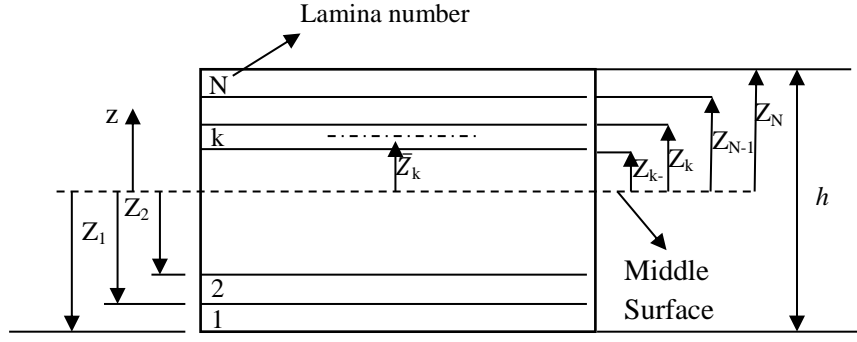
23

**Figure 3.6** Geometrical shape of a laminate

$$\begin{Bmatrix} N_x \\ N_y \\ N_{xy} \end{Bmatrix} = \sum_{k=1}^{N} \int_{z_{k-1}}^{z_k} \begin{Bmatrix} \sigma_x \\ \sigma_y \\ \sigma_{xy} \end{Bmatrix}^k dz$$

(3.90)

$$\begin{Bmatrix} M_x \\ M_y \\ M_{xy} \end{Bmatrix} = \sum_{k=1}^{N} \int_{z_{k-1}}^{z_k} \begin{Bmatrix} \sigma_x \\ \sigma_y \\ \sigma_{xy} \end{Bmatrix}^k z dz$$

(3.91)

$$\begin{Bmatrix} V_y \\ V_x \end{Bmatrix} = \sum_{k=1}^{N} \int_{z_{k-1}}^{z_k} \begin{Bmatrix} \sigma_{yz} \\ \sigma_{xz} \end{Bmatrix}^k z dz$$

(3.92)

Where $\sigma_x$, $\sigma_y$, $\sigma_{xy}$, $\sigma_{yz}$ and $\sigma_{xz}$ are stress components of the plate. Constitutive equation containing of forces, moments, strains and curvatures can be expressed as in the form of the matrix by using (3.90), (3.91) and (3.92)

$$\begin{bmatrix} N_{xx} \\ N_{yy} \\ N_{xy} \\ M_{xx} \\ M_{xx} \\ M_{xy} \end{bmatrix} = \begin{bmatrix} A_{11} & A_{12} & A_{16} & B_{11} & B_{12} & B_{16} \\ A_{12} & A_{22} & A_{26} & B_{21} & B_{22} & B_{26} \\ A_{16} & A_{26} & A_{33} & B_{16} & B_{26} & B_{66} \\ B_{11} & B_{12} & B_{16} & D_{11} & D_{12} & D_{16} \\ B_{21} & B_{22} & B_{26} & D_{12} & D_{11} & D_{26} \\ B_{16} & B_{26} & B_{66} & D_{16} & D_{26} & D_{33} \end{bmatrix} \begin{bmatrix} \varepsilon_{xx}^0 \\ \varepsilon_{yy}^0 \\ \varepsilon_{xy}^0 \\ \kappa_{xx} \\ \kappa_{yy} \\ \kappa_{xy} \end{bmatrix}$$

(3.93)

Where $[A]_{ij}$ is in-plane stiffness matrix which depends on in plane strains and forces, $[D]_{ij}$ is bending stiffness matrix which depends on curvatures and bending moments,

$[B]_{ij}$ is bending-extension coupling matrix that it relates in plane strains to bending moments

$$[A]_{ij} = \sum_{k=1}^{N} \left(\overline{Q}_{ij}\right)_k \left(z_k - z_{k-1}\right)$$

(3.94)

$$[B]_{ij} = \frac{1}{2} \sum_{k=1}^{N} \left(\overline{Q}_{ij}\right)_k \left(z_k^2 - z_{k-1}^2\right)$$

(3.95)

$$[D]_{ij} = \frac{1}{3} \sum_{k=1}^{N} \left(\overline{Q}_{ij}\right)_k \left(z_k^3 - z_{k-1}^3\right)$$

(3.96)

Where $\overline{Q}_{ij}$ is the inverse of reduced stiffness matrix.

Moment and force equations with respect to the neutral plane were reduced to following matrix because of extension and bending coupling stiffness matrix $[B]_{ij}$ was zero from symmetry [31].

$$\begin{bmatrix} N_{xx} \\ N_{yy} \\ N_{xy} \\ M_{xx} \\ M_{xx} \\ M_{xy} \end{bmatrix} = \begin{bmatrix} A_{11} & A_{12} & 0 & 0 & 0 & 0 \\ A_{12} & A_{22} & 0 & 0 & 0 & 0 \\ 0 & 0 & A_{33} & 0 & 0 & 0 \\ 0 & 0 & 0 & D_{11} & D_{12} & 0 \\ 0 & 0 & 0 & D_{12} & D_{11} & 0 \\ 0 & 0 & 0 & 0 & 0 & D_{33} \end{bmatrix} \begin{bmatrix} \varepsilon_{xx}^0 \\ \varepsilon_{yy}^0 \\ \varepsilon_{xy}^0 \\ \kappa_{xx} \\ \kappa_{yy} \\ \kappa_{xy} \end{bmatrix}$$

(3.97)

Explicit form of moment equations are as follows

$$M_{xx} = D_{11}\kappa_{xx} + D_{12}\kappa_{yy}$$

(3.98)

$$M_{yy} = D_{12}\kappa_{xx} + D_{22}\kappa_{yy}$$

(3.99)

$$M_{xy} = D_{33}\kappa_{xy}$$

(3.100)

Substituting (3.98), (3.99) and (3.100) in the (3.13) gives

$$\left( D_{11} \frac{\partial^2 \kappa_{xx}}{\partial x^2} + D_{12} \frac{\partial^2 \kappa_{yy}}{\partial y^2} \right) + 2D_{33} \frac{\partial^2 \kappa_{xy}}{\partial x \partial y} + \left( D_{12} \frac{\partial^2 \kappa_{xx}}{\partial y^2} + D_{22} \frac{\partial^2 \kappa_{yy}}{\partial y^2} \right) = \rho h \frac{\partial^2 w}{\partial t^2}$$

(3.101)

Where

$$\kappa_{xx} = -\frac{\partial^2 w}{\partial x^2} \qquad (3.102)$$

$$\kappa_{yy} = -\frac{\partial^2 w}{\partial y^2} \qquad (3.103)$$

$$\kappa_{xy} = -\frac{\partial^2 w}{\partial x \partial y} \qquad (3.104)$$

Substituting (3.102), (3.103) and (3.104) in the (3.101) gives

$$D_{11}\frac{\partial^4 w}{\partial x^4} + 2(D_{12} + 2D_{33})\frac{\partial^4 w}{\partial x^2 \partial y^2} + D_{22}\frac{\partial^4 w}{\partial y^4} = \rho h \frac{\partial^2 w}{\partial t^2} \qquad (3.105)$$

Exact solution of equation (3.105) can be obtained as equation (3.106) by substituting a function of $w(x, y, t) = W(x, y)\sin(\omega t)$ in the equation (3.105) and by applying simply supported boundary condition to the edge of the plate

$$\omega_{mn} = \pi^2 \sqrt{D_{11}\left(\frac{m}{a}\right)^4 + 2(D_{12} + 2D_{33})\left(\frac{m}{a}\right)^2\left(\frac{m}{b}\right)^2 + D_{22}\left(\frac{n}{b}\right)^4} \sqrt{\frac{1}{\rho h}} \qquad (3.106)$$

26

# CHAPTER 4

# EXPERIMENTAL STUDIES

## 4.1 Materials and Method

Hybrid composites are constituted of at least two successive layers made of fibers of different mechanical properties such as Glass, Carbon and Kevlar fibers... etc. Since each fiber has different mechanical properties, it is necessary to show effects of the nature of fiber in the layers for predicting of dynamic behavior of hybrid composite laminates.

In experimental studies, hybrid composite plates were fabricated with 12 layers. Woven Carbon, Kevlar and S-Glass fibers were used as reinforcements. Laminated fabrics were laid on the flat mold and subjected to 0.3 MPa pressure for 1 hour curing time with 90 $^{0}$C under press. Fibers were fabricated with 240x350 mm dimensions; epoxy resin was prepared by mixing of epoxy with hardener. Adequate epoxy resin was put on the surface of the first layer and uniformly distributed by the application of roller through surface of the fiber as seen in Figure 4.1 (b). This process was continued for all layers. Produced hybrid composite specimens were cut in the desired dimensions of 200x200 mm. Some of produced hybrid composite materials and fibers were shown in Figure 4.1. An epoxy resin (MOMENTIVE-MGS L285), a hardener as catalyst (MOMENTIVE-MGS H285) and a releasing agent (Dost Kimya-OZ 5111) were used in production of hybrid composites.

Stacking sequences and fiber configurations of produced test specimens were given in Table 4.1
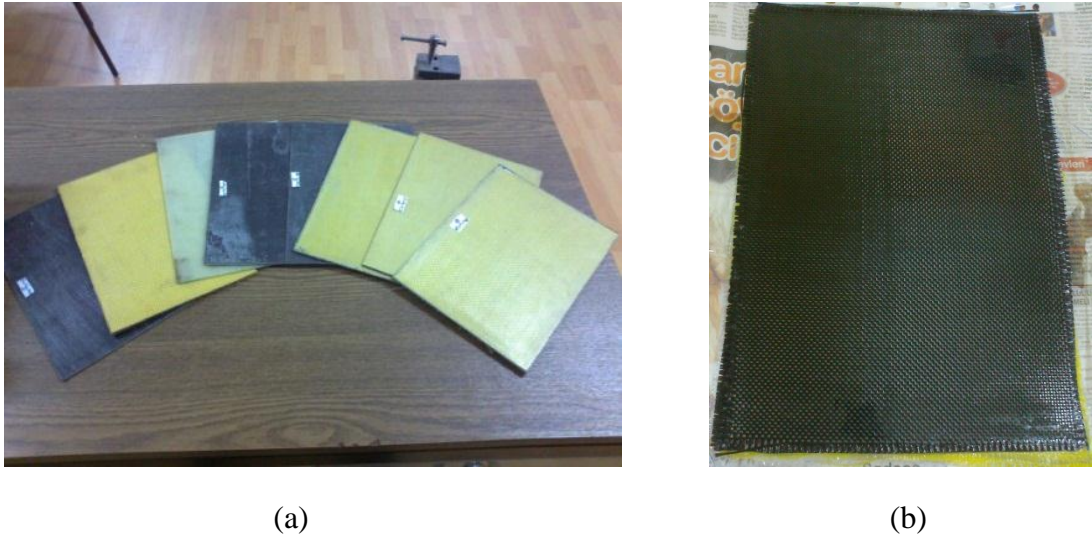


(a)                                                    (b)

**Figure 4.1** Hybrid composite materials. (a) Hybrid composite plates, (b) Fabric fibers

**Table 4.1** Lay-up sequence of produced specimens

| Material Number | Lay-up sequence |
|:---:|:---:|
| 1 | $[(0°_K/90°_K)_3]_S$ |
| 2 | $[(0^0_K/90^0_K)/(0^0_C/90^0_C)/(0^0_G/90^0_G)]_S$ |
| 3 | $[(0°_K/90°_K)/(0°_G/90°_G)/(0°_C/90°_C)]_S$ |
| 4 | $[(0°_C/90°_C)/(0°_K/90°_K)/(0°_G/90°_G)]_S$ |
| 5 | $[(0°_C/90°_C)_3]_S$ |
| 6 | $[(0°_C/90°_C)/(0°_G/90°_G)/(0°_K/90°_K)]_S$ |
| 7 | $[(0°_G/90°_G)/(0°_K/90°_K)/(0°_C/90°_C)]_S$ |
| 8 | $[(0°_G/90°_G)/(0°_C/90°_C)/(0°_K/90°_K)]_S$ |
| 9 | $[(0°_G/90°_G)_3]_S$ |

## 4.2 Mechanical Properties of Specimens

An experimental set-up was used to determine mechanical properties of fabricated test specimens as shown in Figure 4.2.
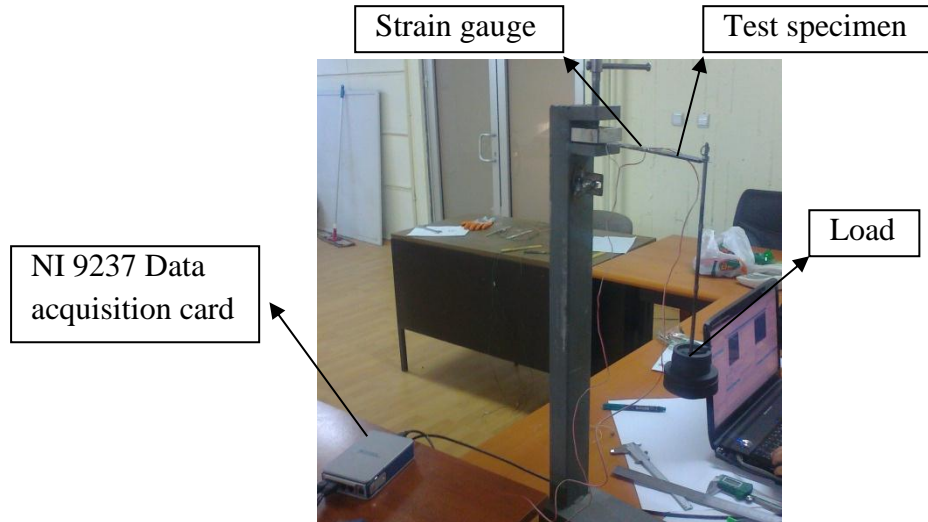


**Figure 4.2** Experimental set-up

It is essential here to determine mechanical properties of Carbon/Epoxy, Kevlar/Epoxy and S-Glass/Epoxy since all of produced hybrid composite specimens contain combinations of S-Glass, Kevlar and Carbon fibers. Some of prepared test specimens are shown in Figure 4.3. Mechanical properties of Carbon/Epoxy, Kevlar/Epoxy and S-Glass/Epoxy materials were determined experimentally as listed in Table 4.2
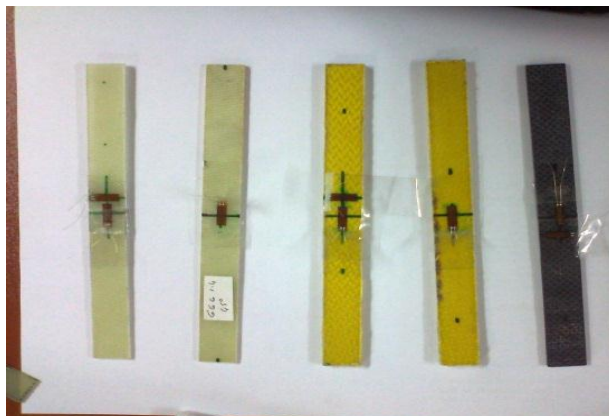


**Figure 4.3** Test specimens for strain gauge experiment

**Table 4.2** Mechanical properties of produced test specimens

| Material lay-up sequence | $E_{12} = E_{21}$ (Gpa) | $\upsilon_{12} = \upsilon_{21}$ | $G_{12} = G_{21}$ (Gpa) | $\rho(kg/m^3)$ |
|---|---|---|---|---|
| S-Glass/Epoxy | 19.5 | 0.15 | 3.7 | 1710 |
| Carbon/Epoxy | 49 | 0.10 | 3.2 | 1440 |
| Kevlar/Epoxy | 26.5 | 0.09 | 1.5 | 1250 |

## 4.3 Experimental Modal Analysis

Bridges, aircraft wings, wind turbines and any other structures have natural frequencies. When the natural frequency is excited, the structure resonates. The amplitude of vibration will increase significantly, thus the stress of the structure increase significantly. The increased stress reduces the life of the machine component and structures. Therefore it is important to determine natural frequency and eliminate it for safety design of the system.

Experimental modal analysis is one of the most commonly used method to show natural characteristic of the system such as frequency, damping and mode shapes. In this section, Experimental Modal Analysis (EMA) was presented in detail by introducing Frequency Response Function (FRF)

## 4.3.1 Frequency Response Function (FRF)

FRF is structural response to an applied input force as a function of frequency which indicate natural characteristics of the excited structures. It performs as a transfer function from the time domain to the frequency domain. The dynamic response of the system may be obtained in terms of displacement, velocity or acceleration by introducing FRF curve. Consider a linear system as given in Figure 4.4. FRF was obtained in terms of acceleration X ($\omega$) by the application of input fore F ($\omega$) and transfer function of H ($\omega$). Relationship between input and output functions was expressed as [32]

$$X(\omega) = F(\omega) H(\omega) \tag{4.1}$$

$$H(\omega) = \frac{X(\omega)}{F(\omega)}$$

(4.2)

Input Force                               Acceleration Response

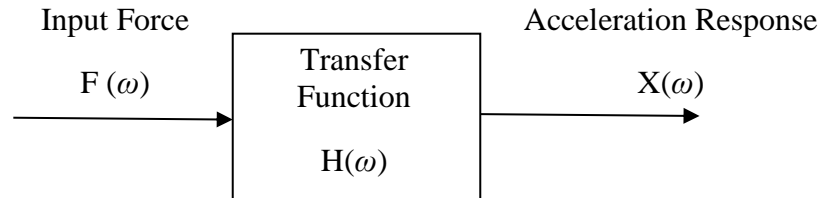$F(\omega)$             Transfer Function             $X(\omega)$

$H(\omega)$

**Figure 4.4** FRF of the linear system

### 4.3.2 Impact Testing

Impact testing method is most popular technique today to measure vibration characteristics of the machines and structures because of very convenient, fast and low cost. Impact testing is simulated as shown in Figure 4.5. Main requirements for impact testing method are

- An *impact hammer* with a load cell to measure the input force

- An *accelerometer* to measure the response of the given input force

- A 2 or 4 channel *FFT analyzer* or *Data Acquisition Card (DAQ)*

- A suitable *modal analysis software*
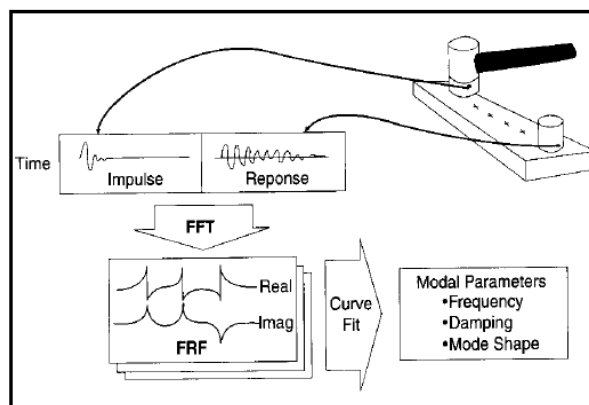


**Figure 4.5** Impact testing method

## 4.4 Experimental Set-up

An experimental set-up for modal analysis was used to determine damping ratios and natural frequencies of hybrid composite plates under the SS-F-SS-F, C-F-C-F and C-F-F-F boundary conditions. An accelerometer for output signal acquisition, an impact hammer for stimulus force signal, data acquisition card and a suitable software for modal analysis were used in the modal analysis as seen in Figure 4.6.
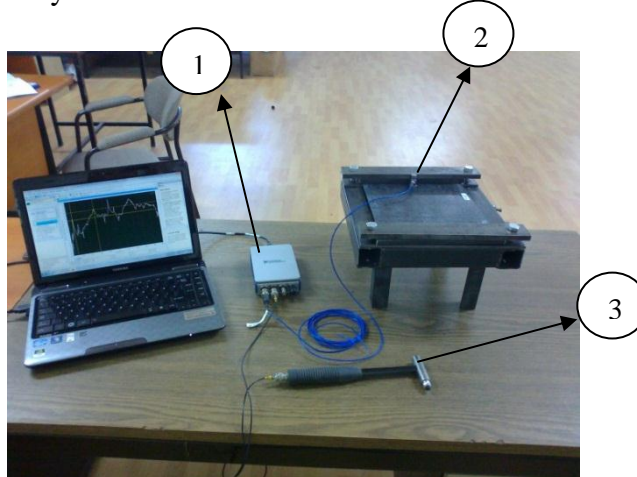


**Figure 4.6** Experimental modal analysis set-up. (1) Data acquisition card, (2) Accelerometer, (3) Modal impact hammer

## 4.4.1 Accelerometer PCB 352C03

General purpose, PCB 352C03 ceramic shear ICP® accelerometer device was used for sensing vibration frequencies of test the specimens once the excitation was begun by the application of impact hammer on the test specimens as shown in the Figure 4.7. Its main features are given in Table 4.3



**Figure 4.7** PCB 352C03 Ceramic shear accelerometer

**Table 4.3** Main features of ICP® accelerometer

| | | |
|---|---|---|
| Sensitivity (± 10 %) | 10 mV/g | 1.02 mV/(m/s²) |
| Measurement Range | ± 500 g pk | ± 4900 m/s² pk |
| Frequency Range (± 5 %) | 0.5 to 10,000 Hz | 0.5 to 10,000 Hz |
| Frequency Range (± 10 %) | 0.3 to 15,000 Hz | 0.3 to 15,000 Hz |
| Resonant Frequency | ≥ 50 kHz | ≥ 50 kHz |
| Broadband Resolution (1 to 10,000 Hz) | 0.0005 g rms | 0.005 m/s² rms |
| Non-Linearity | ≤ 1 % | ≤ 1 % |
| Transverse Sensitivity | ≤ 5 % | ≤ 5 % |

### 4.4.2 Modal Impact Hammer PCB 086C03

PCB 086C03 general purpose modal impact hammer was used in  order to provide stimulus input force signal to the plate for the excitation as seen in Figure 4.8. Variable impact hammer tips were used in order to better amplitude and band-width of excitation. Main properties of the modal impact hammer were given in the Table 4.4



**Figure 4.8** PCB 086C03 modal impact hammer

**Table 4.4** Properties of modal impact hammer

| | |
|---|---|
| Sensitivity (± 15 %) | 2.25 mV/N |
| Measurement Range | ± 2224 N pk |
| Resonant Frequency | ≥ 22 kHz |
| Non-Linearity | ≤ 1 % |

### 4.4.3 Data Acquisition Card (DAQ)

The main function of the DAQ is to receive time varying data kept from accelerometer and impact hammer and convert it to the frequency based signals. National Instrument product NI 9234 data acquisition device was used for modal analysis testing as shown in Figure 4.9



**Figure 4.9** Data acquisition card (DAQ)

Specific functions of NI 9234 DAQ are

- 24-bit resolution

- 102 dB dynamic range

- 4 simultaneous analog inputs

- ±5 V input range

- Antialiasing filters

- TEDS read/write

- Supported in NI CompactDAQ, CompactRIO, and Hi-Speed USB carrier

## 4.5 Experimental Procedure

➢ Manufactured test specimens were fixed in the frame as required boundary condition, C-F-C-F, C-F-F-F or SS-F-SS-F

➢ Accelerometer was fixed on the surface of the test specimens near the fixed edge

➢ Both impact hammer and accelerometer were connected as an analog input to DAQ by connection cables

➢ LABVIEW software was run in order to plot FRF on monitor

➢ Impact hammer was struck four or five times on the plate for better excitation. Struck points were shown in Figure 4.10

➢ FRF and time signal graph were plotted on a computer by using LABVIEW software
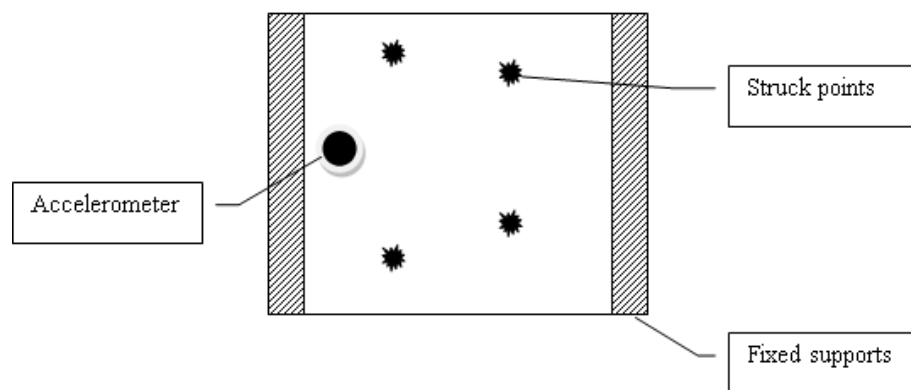


**Figure 4.10** Modal impact hammer excitation points for C-F-C-F boundary condition

Natural frequencies were plotted on the screen from FRF curves by the application of modal impact hammer as shown in Figure 4.11. First two natural frequencies of hybrid composites were measured as given in Table 4.5
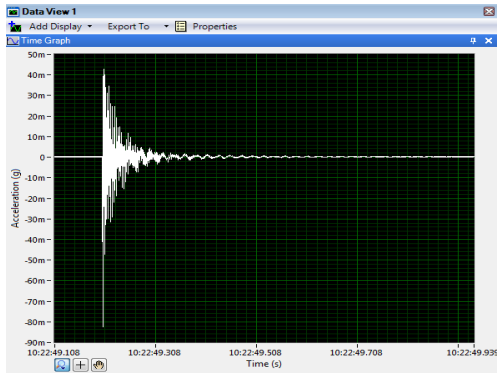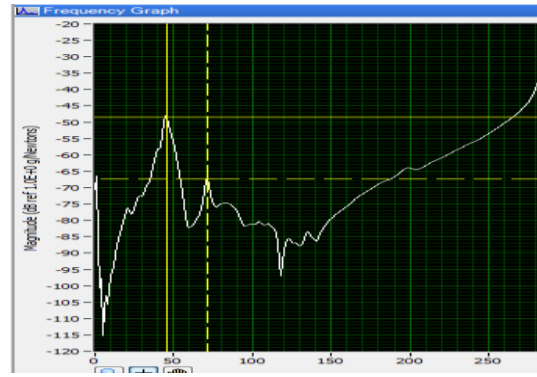
(a)                                                                                    (b)

**Figure 4.11** (a) Time decaying graph of material 2 under the C-F-F-F case, (b) Frequency response graph of material 2 under the C-F-F-F case

**Table 4.5** First two natural frequencies of hybrid composite plates

| Material | C-F-C-F | | C-F-F-F | | SS-F-SS-F | |
|---|---|---|---|---|---|---|
| Number | Mode 1 (Hz) | Mode 2 (Hz) | Mode 1 (Hz) | Mode 2 (Hz) | Mode 1 (Hz) | Mode 2 (Hz) |
| 1 | 298.29 | 337.28 | 50.77 | 70.43 | 150.51 | 165.92 |
| 2 | 319.60 | 345.67 | 52.13 | 72.19 | 157.53 | 175.67 |
| 3 | 266.56 | 285.06 | 44.61 | 69.65 | 128.38 | 154.50 |
| 4 | 344.14 | 386.71 | 61.50 | 84.45 | 173.84a | 188.69 |
| 5 | 370.81 | 427.43 | 62.17 | 99.18 | 173.19 | 199.84 |
| 6 | 337.66 | 370.48 | 52.76 | 90.28 | 177.03 | 199.31 |
| 7 | 262.93 | 289.00 | 41.93 | 73.67 | 119.85 | 152.19 |
| 8 | 286.03 | 323.81 | 46.41 | 85.27 | 145.71 | 162.98 |
| 9 | 224.15 | 263.19 | 36.52 | 70.52 | 115.41 | 145.07 |

## 4.6 Damping Ratio (Half-power bandwidth method)

Half-power bandwidth method is the most common method for determining damping ratio. Firstly maximum amplitude of $n^{th}$ mode frequency was determined from the frequency response curve, $\omega_1$ and $\omega_2$ frequencies corresponding to $Z_1$ and $Z_2$ points were found by dividing maximum amplitude of $n^{th}$ mode in the $\sqrt{2}$ as shown in Figure 4.12.

$$\xi = \frac{\omega_2 - \omega_1}{2\omega_n} \tag{4.3}$$

Where $\xi$ is the damping ratio, $\omega_n$ is the natural frequency of $n^{th}$ mode and $\omega_2 - \omega_1$ is the bandwidth.
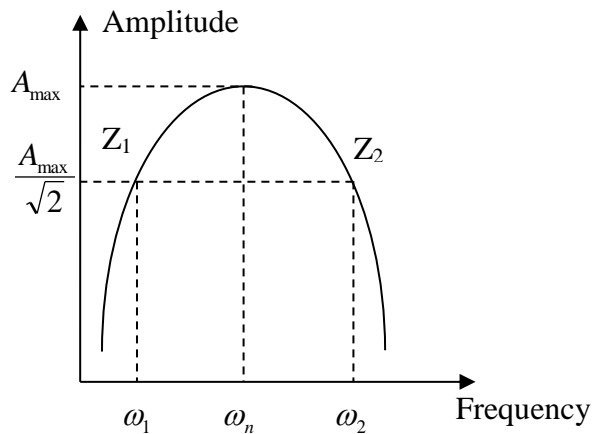


**Figure 4.12** Half-power bandwidth method

Damping ratio of the hybrid composite plates was given in Figure 4.13. As can be seen in Figure 4.13, the maximum damping ratio was obtained from Kevlar/Epoxy and the minimum damping ratio was obtained from Carbon/Epoxy. It was also reported here that damping ratio was decreased by the increasing in natural frequencies.
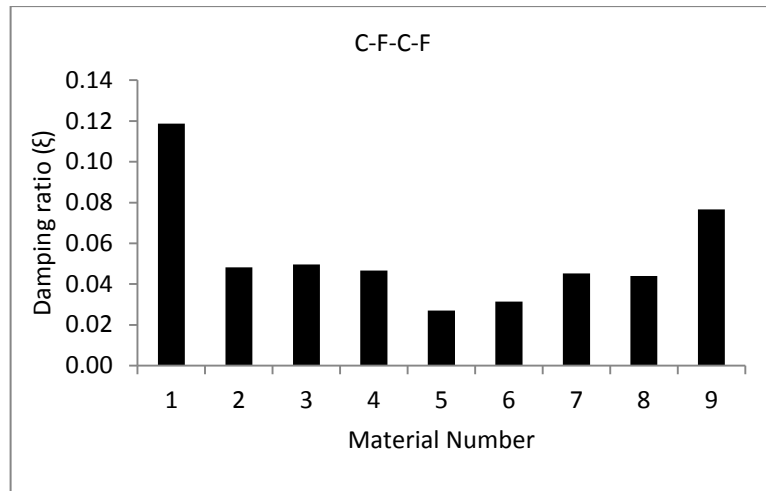
(a)
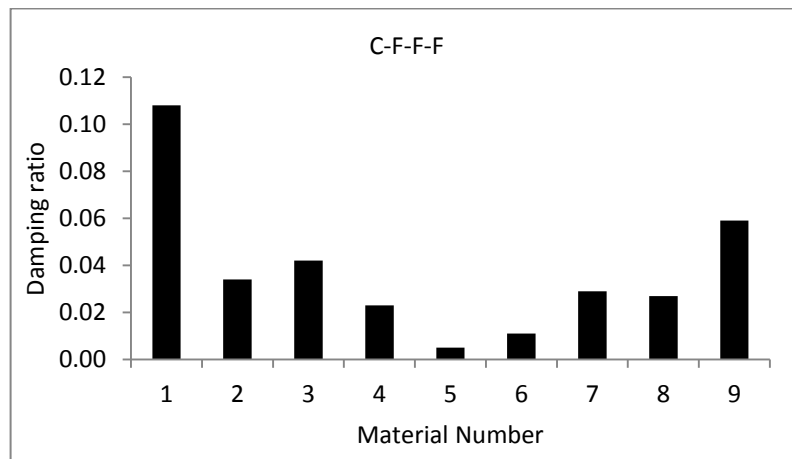


(b)
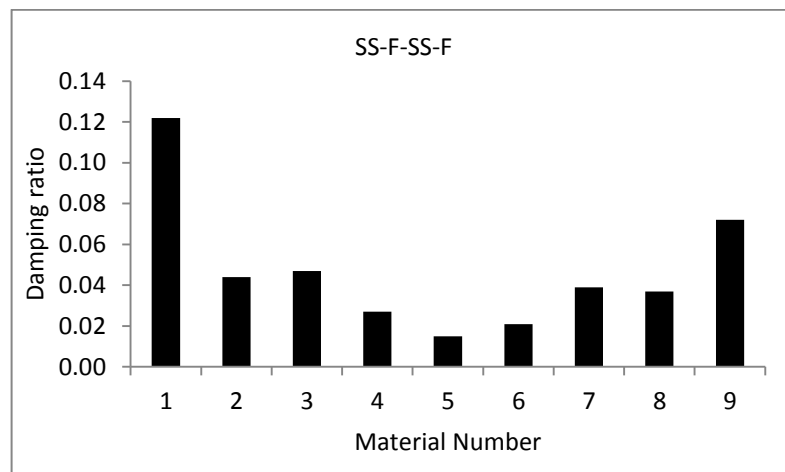


(c)

**Figure 13** Damping ratios of hybrid composite plates. (a) C-F-C-F, (b) C-F-F-F, (c) SS-F-SS-F boundary condition

# CHAPTER 5

## FINITE ELEMENT MODELLING

Finite element modeling (FEM) is powerful tool for solution of many engineering problems. The prime objective of the FEM is to represent the behavior of the physical system in static, dynamic, thermal, buckling and vibration conditions.

ANSYS 12.1 software was used in numerical studies in order to predict dynamic behaviors of hybrid composite plates in the extended mode range. 1600 elements were used in the finite element model. Linear layer element SHELL 99 which has 6 degrees of freedom at each node, translation in x-, y-, z- and rotation in x-, y-, z- directions as shown in Figure 5.1. Numerical results were given in Table 5.1.
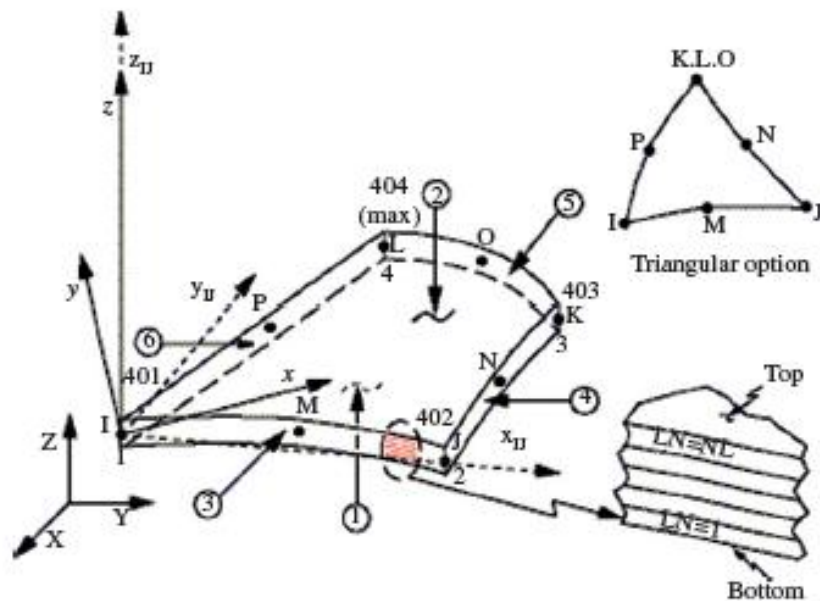


**Figure 5.1** The element of SHELL 99 [33]

**Table 5.1** Numerical results (a) C-F-C-F, (b) C-F-F-F, (c) SS-F-SS-F

| Mode Number | 1 | | | 2 | | |
|---|---|---|---|---|---|---|
| Material Number | Exp. | ANSYS | %Diff. | Exp. | ANSYS | %Diff. |
| 1 | 298.29 | 320.76 | 7.53 | 337.28 | 331.16 | -1.65 |
| 2 | 319.60 | 326.73 | 2.23 | 345.67 | 338.52 | -2.07 |
| 3 | 266.56 | 292.01 | 9.55 | 285.06 | 305.75 | 7.26 |
| 4 | 344.14 | 373.58 | 8.55 | 386.71 | 387.68 | 0.25 |
| 5 | 370.81 | 406.83 | 9.71 | 427.43 | 422.02 | -1.27 |
| 6 | 337.66 | 366.91 | 8.66 | 370.48 | 383.59 | 3.54 |
| 7 | 262.93 | 274.35 | 4.34 | 289.00 | 295.06 | 2.10 |
| 8 | 286.03 | 303.00 | 5.93 | 323.81 | 324.10 | 0.09 |
| 9 | 224.15 | 237.78 | 6.08 | 263.19 | 261.74 | -0.55 |

(a)

| Mode Number | 1 | | | 2 | | |
|---|---|---|---|---|---|---|
| Material Number | Exp. | ANSYS | %Diff. | Exp. | ANSYS | %Diff. |
| 1 | 50.77 | 50.77 | -0.01 | 70.43 | 70.51 | 0.11 |
| 2 | 52.13 | 51.59 | -1.05 | 72.19 | 73.46 | 1.73 |
| 3 | 44.61 | 46.06 | 3.15 | 69.65 | 70.17 | 0.74 |
| 4 | 61.50 | 59.07 | -4.11 | 84.45 | 85.02 | 0.67 |
| 5 | 62.17 | 64.33 | 3.36 | 99.18 | 92.37 | -7.37 |
| 6 | 52.76 | 58.00 | 9.04 | 90.28 | 87.57 | -3.09 |
| 7 | 41.93 | 43.24 | 3.02 | 73.67 | 75.73 | 2.72 |
| 8 | 46.41 | 47.79 | 2.88 | 85.27 | 81.61 | -4.48 |
| 9 | 36.52 | 37.42 | 2.41 | 70.52 | 72.16 | 2.27 |

(b)

| Mode Number | 1 | | | 2 | | |
|---|---|---|---|---|---|---|
| Material Number | Exp. | ANSYS | %Diff. | Exp. | ANSYS | %Diff. |
| 1 | 150.51 | 142.05 | 5.62 | 165.92 | 160.23 | -3.55 |
| 2 | 157.53 | 144.37 | 8.36 | 175.67 | 164.84 | -6.57 |
| 3 | 128.38 | 128.87 | -0.38 | 154.50 | 152.34 | -1.42 |
| 4 | 173.84 | 165.30 | 4.91 | 188.69 | 189.67 | 0.52 |
| 5 | 173.19 | 180.02 | -3.94 | 199.84 | 206.33 | 3.15 |
| 6 | 177.03 | 162.28 | 8.33 | 199.31 | 190.81 | -4.45 |
| 7 | 119.85 | 120.93 | -0.90 | 152.19 | 155.13 | 1.90 |
| 8 | 145.71 | 133.68 | 8.26 | 162.98 | 168.73 | 3.41 |
| 9 | 115.41 | 120.93 | -4.78 | 145.07 | 155.13 | 6.48 |

(c)
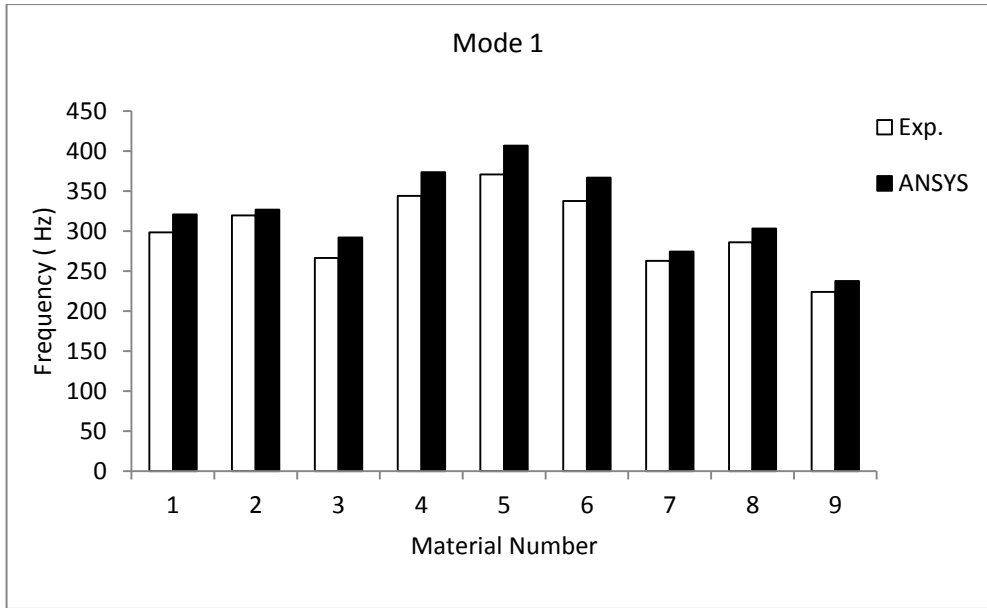
(a)
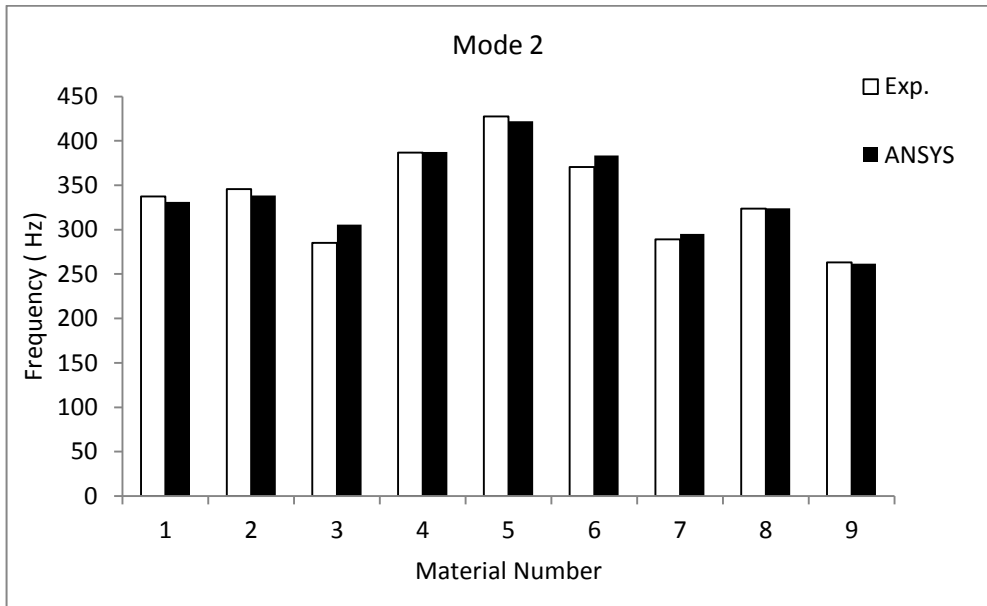


(b)

**Figure 5.2** Experimental and ANSYS results for square plates under the C-F-C-F edge condition. (a) Natural frequency in mode 1. (b) Natural frequency in mode 2
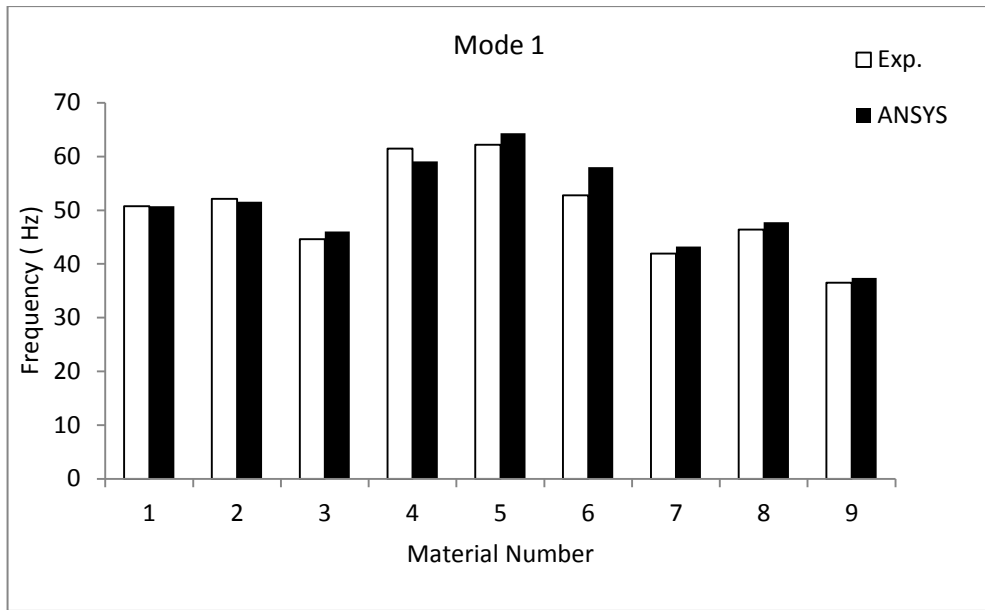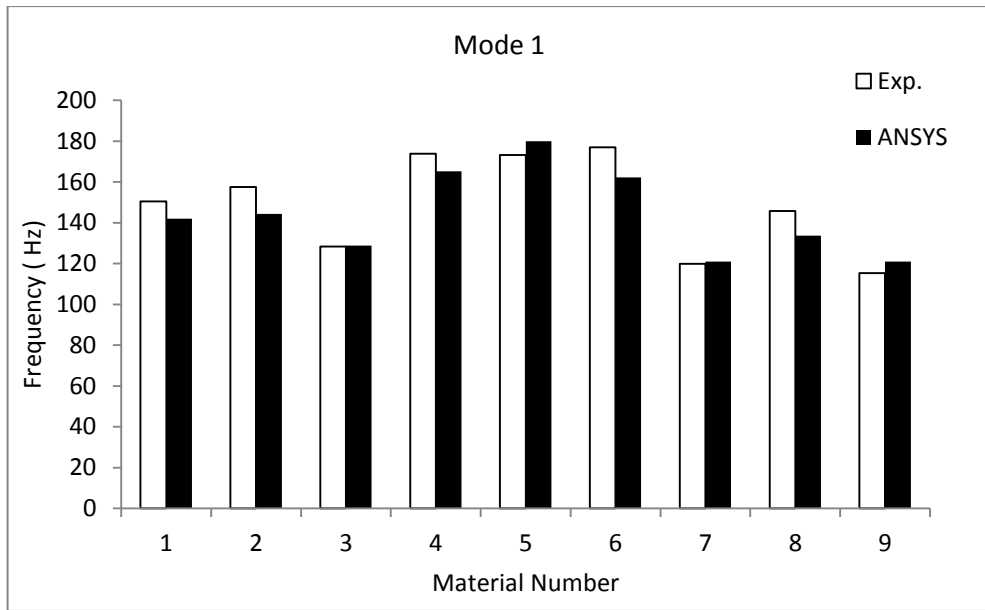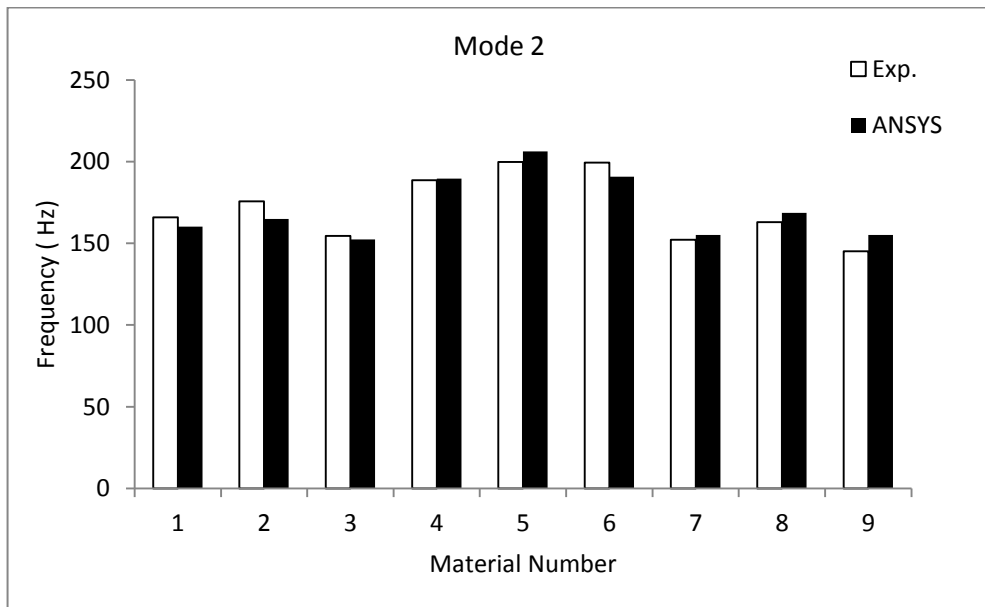
(a)
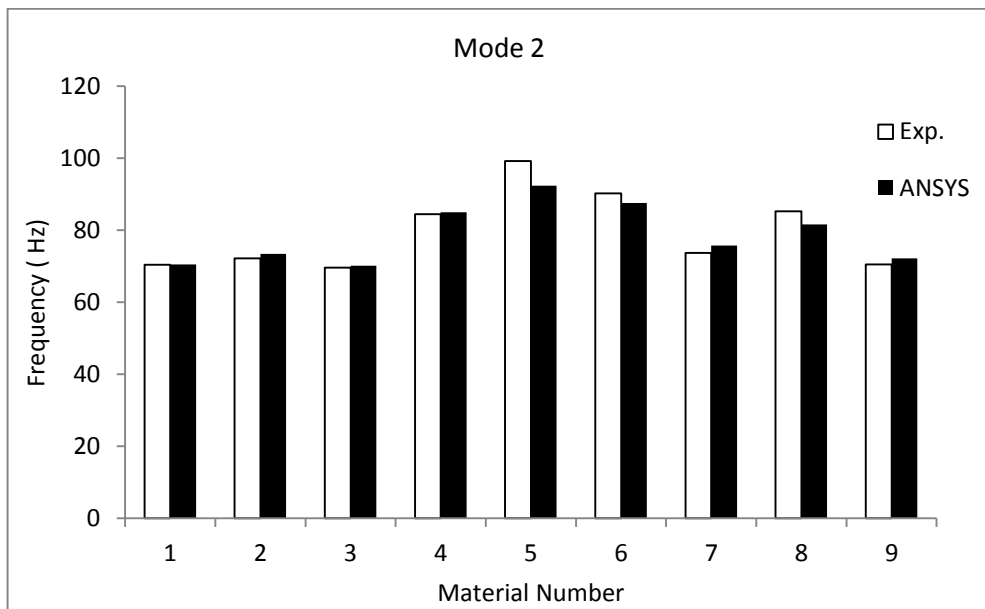


(b)

**Figure 5.3** Experimental and ANSYS results for square plates under the C-F-F-F edge condition. (a) Natural frequency in mode 1. (b) Natural frequency in mode 2

(a)



(b)

**Figure 5.4** Experimental and ANSYS results for square plates under the SS-F-SS-F edge condition. (a) Natural frequency in mode 1. (b) Natural frequency in mode 2
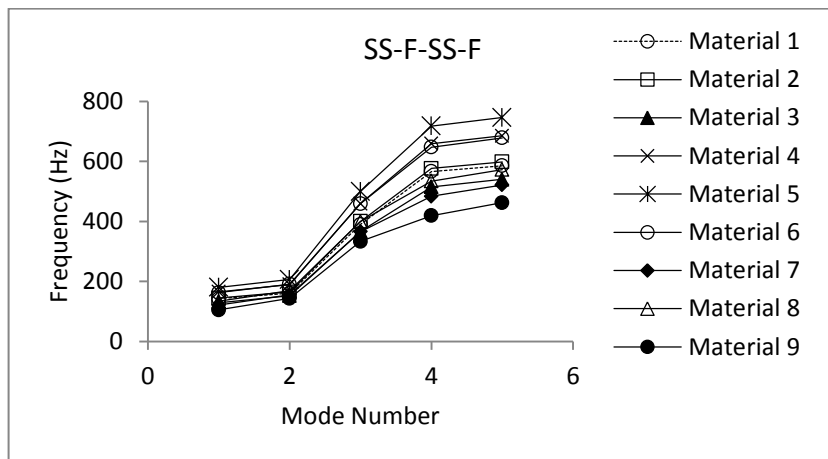
As can be seen in Table 5.1, Figure 5.2, Figure 5.3 and Figure 5.4, ANSYS finite element results were in close agreement with experimental results. Numerical studies were extended for first five modes in order to investigate natural frequency distrubutions in higher modes. Figure 5.5 shows numerical results of first five modes.
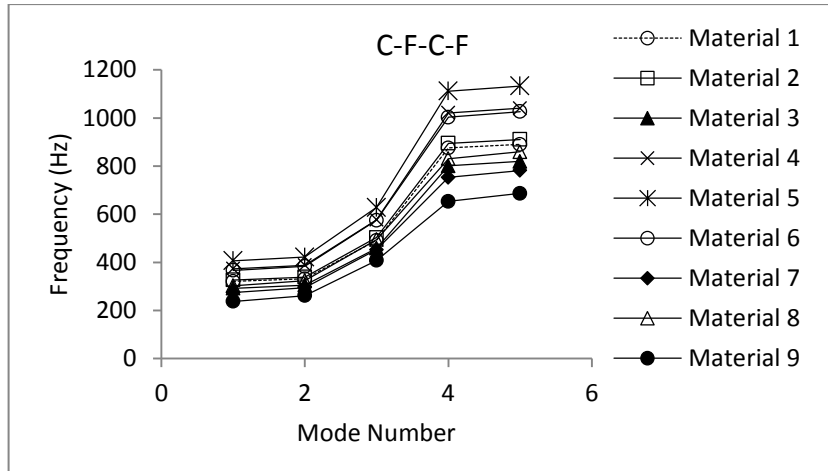
(a)
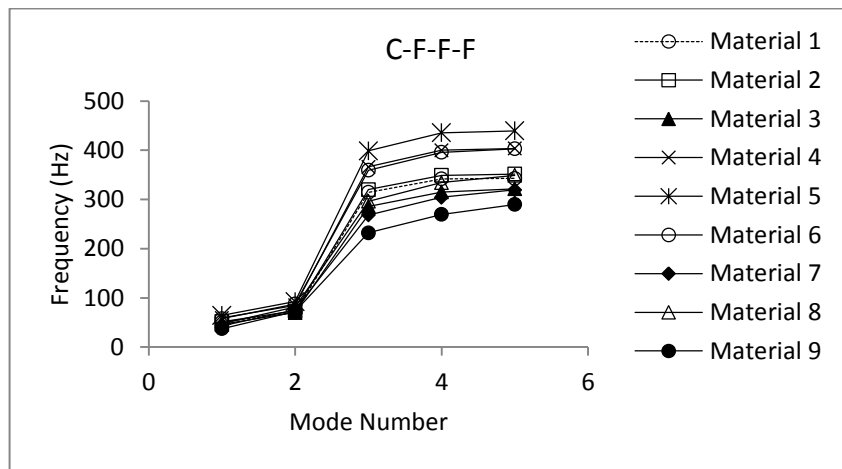


(b)



(c)

**Figure 5.5** First five natural frequencies of produced test specimens. (a) C-F-C-F, (b) C-F-F-F, (c) SS-F-SS-F

Although behavior of curves continues in the same way in the high modes, difference between frequencies of the materials are increased. Maximum natural frequency was determined in material 5 due to ratio of Carbon fiber and minimum frequency was determined in material 9 due to ratio of Glass fiber. It can be easily seen in Figure 5.5, if Carbon ratio is increased in the laminate, natural frequency is also increasing due to stiffness of the Carbon fiber.
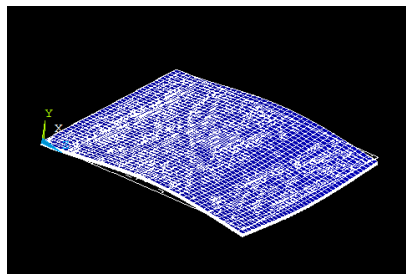
Mode shapes of material 2 were given in Figure 5.6 for C-F-F-F boundary condition. As seen from Figure 5.6, first, third and fourth modes are bending mode, other modes are twisting mode.
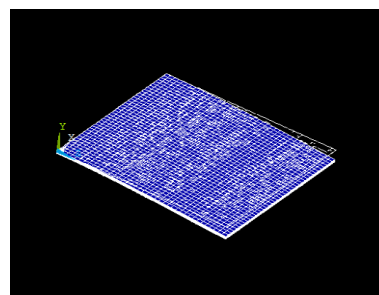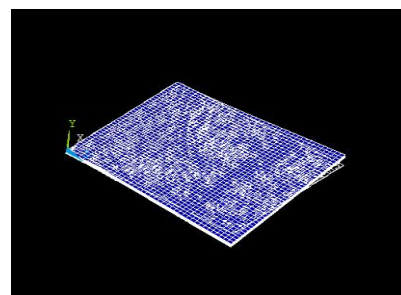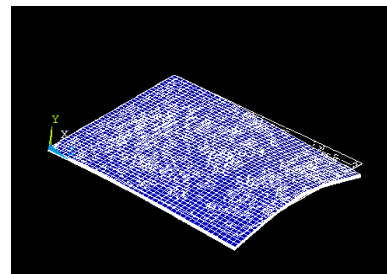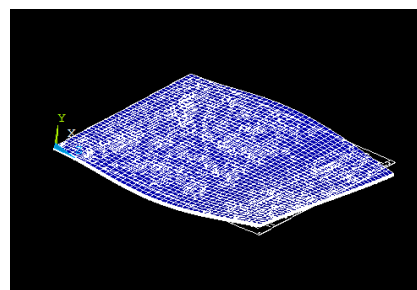


Mode 1 (51.59 Hz)          Mode 2 (73.46 Hz)



Mode 3 (319.98 Hz)          Mode 4 (348.86 Hz)



Mode 5 (351.52 Hz)

**Figure 5.6** Mode shape plots of material 2 for C-F-F-F boundary condition

# CHAPTER 6

## RESULTS AND CONCLUSION

In this study, effects of fiber type and fiber combinations in a lamina on the natural frequencies and damping properties of the hybrid composite plates were investigated with various boundary conditions. Carbon, Kevlar and S-Glass fibers were used as reinforcements. Experimental studies were carried out to determine natural frequencies and damping values. In addition, numerical studies were performed for validation of experimental results. It was concluded  that both experimental and numerical results were in close agreement with each other. Main conclusions from this study can be drawn as follows;

- Natural frequencies and damping properties of laminated hybrid composite plates are considerably affected by boundary conditions. The maximum and minimum frequency values were recorded in C-F-C-F and C-F-F-F edge conditions, respectively,

- For all modes, material 9 with stacking sequence of $[(0°_G/90°_G)_3]_S$ had minimum natural frequency than other materials due to lower bending stiffness of the S-glass fiber,

- For all modes, material 5 with stacking sequence of $[(0°_C/90°_C)_3]_S$ had maximum natural frequency than other materials due to higher bending stiffness of carbon fibers,

- Natural frequencies of laminated hybrid composite plates in higher modes are considerably effected by replacements of Kevlar, Carbon and Glass fibers in the layers,

- Minimum natural frequency of laminated hybrid composite plates was detected by material 7 with stacking sequence of $[(0°_G/90°_G)/(0°_K /90°_K)/(0°_C /90°_C)]_S$ ,

- Natural frequencies are increased by the use of fibers which have higher stiffness in the upper layer,

- The maximum and minimum damping ratios were obtained in $[(0°_K/90°_K)_3]_S$ and $[(0°_C/90°_C)_3]_S$ stacking sequences respectively since viscoelastic behavior of Kevlar fiber was significantly greater than Carbon and Glass fiber,

- Damping properties are increased by the use of fibers which have higher viscoelastic property in the upper layer,

- When the damping properties are important for the structural design, Kevlar fiber should be used in the upper layer.

## FUTURE WORKS

- Composite materials that are different than Carbon, Kevlar and S-Glass fibers can be used for combination of different stacking sequence.

- The effects of other boundary conditions on damping and natural frequencies of hybrid composites can be investigated for symmetric and antisymmetric composites

- Damping and free vibration studies can be extended to the stiffened composite plates and shells

# REFERENCES

[1] Barbero, E.J. (2011). *Introduction to composite materials design,*160-215. Boca Raton.

[2] Leissa, W., Qatu., M.S. (2011). *Vibrations of continuous systems,* 1-390. New york.

[3] Leissa, A.W. (1973). The Free Vibration of Rectangular Plates. *Journal of Sound and Vibration.* 31(3), 257-293.

[4] Liew, K.M, Hung, K.C and Lim, M.K. (1995). Three-dimensional vibration of rectangular plates: Effects of thickness and edge constraints. *Journal of Sound and Vibration.* 182 (5), 709–727.

[5] Moon K.K., Sangbo H. (2007). Free vibration analysis of rectangular plate with a hole by means of independent coordinate coupling method. *Journal of Sound and Vibration* 306.

[6] Warburton G.B. (1999). The Vibration of Rectangular Plates. *Journal of Thermoplastic Composite Materials* September 1, 12: 351-372.

[7] Shimpi R.P., Patel H.G. (2006). Free vibrations of plate using two variable refined plate theory. *Journal of Sound and Vibration* 296, 979–999.

[8] Bo, L. and Yufeng, X. (2011). Exact solutions for free in-plane vibrations of rectangular plates. *Acta Mechanica Solida Sinica*, Vol. 24, No. 6.

[9] Jiu, H.W., Liu, A.Q., Chen, H.L. (2007). Exact Solutions for Free-Vibration Analysis of Rectangular Plates Using Bessel Functions. *Journal of Applied Mechanics*, Vol. 74 / 1249.

[10] K. Chandrashekhara, K.Krishnamurthy, S. Royv. (1990). Free vibration of composite beams including rotary inertia and shear deformation. *Composite Structures* Volume 14, Issue 4, Pages 269–279.

[11] Qatu, M.S. (1991). Free Vibration of Laminated Composite Rectangular Plates. *Int. J.Solids Structures*, 28, 941-954.

[12] Narita, Y., Leissa, A.W. (1992). Frequencies and Mode Shapes of Cantilevered Laminated Composite Plates. *Journal of Sound and Vibration*, 154,161-172.

[13] Khdeir, A.A., Reddy, J.N. (1994). Free vibration of cross-ply laminated beams with arbitrary boundary conditions. *International Journal of Engineering Science*, Volume 32, Issue 12, Pages 1971–1980.

[14] Khdeir A.A., Reddy J.N. (1999). Free vibrations of laminated composite plates using second-order shear deformation theory. *Computers and Structures* .71, 617-626.

[15] Won H.L., Sung C.H. (2006). Free and forced vibration analysis of laminated composite plates and shells using a 9-node assumed strain shell element. *Comput. Mech.* 39, 41–58

[16] Aydogdu, M. (2006). Free Vibration Analysis of Angle-ply Laminated Beams with General Boundary Conditions. *Journal of Reinforced Plastics and Composites*, 25:1571.

[17] Mohammed F.A,Goda IGM and Gagal A.H. (2010). *International Journal of Mechanical & Mechatronics* IJMME-IJENS Vol: 10 No: 03.

[18] Cong, D.N., Duy, N.M., Karunasena, W. and Cong., T.T. (2011). Free vibration analysis of laminated composite plates based on FSDT using one-dimensional IRBFN method. *Computers and Structures*, 89, 1–13.

[19] Erklig, A., Bulut, M. and Yeter, E. (2013). Effects of cutouts on natural frequency of laminated composite plates. *Science and Engineering of Composite Materials*. 20(2), 179–185.

[20] Turvey, G.J., Mulcahy, N., Widen, M.B. (2000). Experimental and computed natural frequencies of square pultruded GRP plates: effects of anisotropy, hole size and edge support conditions. *Composite Structures*, 50 391-403.

[21] Itishree, M., Shishir, K.S. (2012). An experimental approach to free vibration response of woven fiber composite plates under free-free boundary condition. *International Journal of Advanced Technology in Civil Engineering*, Volume-1, Issue-2.

[22] Rath, M.K., Sahu, S.K. (2011). Vibration of woven fiber laminated composite plates in hygrothermal environment. *Journal of Vibration and Control* 18(13), 1957–1970.

[23] Adali, S., Verijenko, V.E. (2001). Optimum stacking sequence design of symmetric hybrid laminates undergoing free vibrations. *Composite Stuctures* 54, 131-138.

[24] Idicula, M., Malhotra, S.K., Joseph, M., Thomas, S. (2005). Dynamic mechanical analysis of randomly oriented intimately mixed short banana/sisal hybrid fibre reinforced polyester composites. *Composites Science and Technology* , 65, 1077–1087.

[25] Chen, C. (2005). Investigation on the Vibration and Stability of Hybrid Composite Plates. *Journal of Reinforced Plastics and Composites,* 24, 1747.

[26] Shokrieh, M., Najafi, A. (2006). Experimental evaluation of dynamic behavior of metallic plates reinforced by polymer matrix composites. *Composite Structures,* 75, 472–478.

[27] Botelho, E.C., Campo, A.N., Barros, E., Pardini, L.C., Rezend, M.C. (2006). Damping behavior of continuous fiber/metal composite materials by the free vibration method. Composites: Part B 37 255–263.

[28] Chen, C., Chen, W., Chien, R. (2009). Stability of parametric vibrations of hybrid composite plates. *European Journal of Mechanics A/Solids*, 28 329–337.

[29] Khan, S., Li,C., Siddiqui, AN., Kim, J. (2011). Vibration damping characteristics of carbon fiber-reinforced composites containing multi-walled carbon nanotubes. *Composites Science and Technology*, 71, 1486–1494.

[30] Chakraverty, S. (2009).  Vibrations of plates. 75-200, Boca Raton.

[31] Soedel, W. (2004). Vibrations of shells and plates. 80-403, New york.

[32] Jimin, H., Zhi, F. (2001). Modal analysis. 141-151, Great Britain.

[33] http://ansys.net/old_undocumented/Hlp_E_SHELL99.html.